Mathematics in Applied Sciences and Engineering
Volume **4**, Number **3**, September **2023**, pp.**196-226**
https://ojs.lib.uwo.ca/mase
https://doi.org/10.5206/mase/16474

STEADY-STATE DYNAMICS IN A TWO-PATCH POPULATION MODEL WITH AND WITHOUT ALLEE EFFECT

LAURENCE KETCHEMEN TCHOUAGA AND FRITHJOF LUTSCHER

Abstract. Most biological populations reside in landscapes that consist of many different patches of different quality. Different species differ in their movement behavior, habitat preference and growth rates. Historically, mathematical models for population dynamics have made many simplifying assumptions, such as a single patch or homogeneous landscapes. Recent models have begun to implement landscape heterogeneity and individual movement characteristics, but many of those are based on logistic growth and linear analysis of the zero state. We consider a two-patch model with more general growth functions that can include Allee effects. We prove the existence of steady states and classify their qualitative behavior. In some special cases, we explicitly calculate their stability and use these results to give conditions for when the system exhibits bistability, i.e., the simultaneous existence of two locally stable states. We also study bifurcations with respect to the size of habitat patches and give conditions for forward and backward bifurcations.

1. Introduction

The question of how much space a population requires to persist is an old one in spatial ecology. It dates back to the work by [32] and [19] who determined the conditions for the existence of a positive steady state of a class of reaction–diffusion equations modelling movement and reproduction of a biological population. More specifically, they studied the equation

$$\frac{\partial u}{\partial t} = d\frac{\partial^2 u}{\partial x^2} + h(u), \quad t \geq 0, \tag{1.1}$$

where $u = u(x,t)$ denotes the density of the population at location x and time t with diffusion coefficient d and net growth function $h = h(u)$. They considered a bounded interval $x \in (0, L)$ (the "patch") and so-called hostile boundary conditions $u(0,t) = u(L,t) = 0$. These boundary conditions represent the assumption that individuals who leave the patch are lost from the population and no individuals can enter the patch. They considered a linearly bounded growth function, i.e., $h(u) \leq h'(0)u$, such as the logistic function $h(u) = ru(1-u/K)$. In this case, there exists a positive steady state exactly if the zero steady state is unstable [6]. One can show that this is the case if and only if L is larger than the *minimal patch size* $L^* = \pi\sqrt{d\,h'(0)}$. The minimal patch size indicates a transcritical bifurcation between the zero and positive steady state. This result was later generalized to different boundary conditions (known as mixed or Robin conditions), modelling a boundary where some but not all individuals leave the patch [6]. If no individuals leave the patch, we have the so-called no-flux conditions $u_x(0,t) = u_x(L,t) = 0$, which imply that the population can persist on an arbitrarily small patch.

An *Allee effect* occurs when the per capita population growth rate, $h(u)/u$, is not a monotone decreasing function of density, and a strong Allee effect occurs when the growth rate at low density is

Received by the editors 16 May 2023; accepted 12 September 2023; published online 22 September 2023.
2020 *Mathematics Subject Classification.* Primary 92D40, 35K57; Secondary 35B32, 34B15.
Key words and phrases. Reaction–diffusion system, interface conditions, steady state, population dynamics, Alee effect, Bifurcation.

negative [9]. Many possible mechanisms for an Allee effect exist, for example the difficulty of finding mates or the reduced strength of group defence at low density [9]. When the Allee effect is strong, the zero state is always linearly stable, so that linear stability analysis cannot indicate the existence of a positive steady state. A typical population growth function with strong Allee effect is the cubic function $h(u) = ru(1-u/K)(u/A-1)$ with $0 < A < K$. When this function is used in (1.1), phase-plane methods (see next section) yield a saddle-node bifurcation, where a stable and an unstable positive state exist above a certain critical length, for which no explicit analytical expression exists; see [20] or [6]. In contrast to the case without Allee effect, the population may not persist even with no-flux boundary conditions, if the initial population density is too small.

All of these models consider the case of the single patch of uniform quality, yet, most landscapes consist of several patches of different quality. A typical modelling approach for population dynamics in such multi-patch landscapes consists of using a reaction–diffusion equation of the form in (1.1) on each patch and using matching conditions at the boundary between patches (the "interface") to connect them [3, 2, 7, 8, 12, 17, 16, 21, 23, 25, 24, 26, 28, 30, 31, 36, 27]. Matching conditions represent the movement behavior of individuals, which can include biased movement and habitat preference for particular habitat types. Typically, such conditions impose discontinuities at the interfaces, either in the flux [5] or in the density [25, 28]. The study of the dynamics of such systems has largely focused on the rate of population persistence and spread on steady states when there is no Allee effect. For example, the study of spatial spread in patchy landscapes began with [30] with simple continuity interface conditions until the importance of models details at the interface was discovered [25] and applied to various settings such as marine reserves [2, 21]. Detailed analysis and the existence of spreading speeds and periodic traveling waves were presented recently in [17, 16], while homogenization methods were pioneered in [36]. Steady-state profiles, their stability and potential pattern formation on multi-patch landscapes were investigated in [22, 24, 27]. Models that include an Allee effect are less common since explicit analytical results are rare. The earliest occurrence for a three-patch model is [22], and more recently [26] in an infinite periodic setting and [16] on just two but infinite patches. Unfortunately, there is a huge discrepancy between the few models that include an Allee effect and the increasing acceptance that Allee effects are frequent in nature [9]. There is evidence that the strength of an Allee effect varies spatially [33] and that this variation affects the spreading speed. Since several mechanisms that can cause Allee effects depend on movement and since movement depends on landscape characteristics, it is clear that abiotic heterogeneity can lead to varying strength of Allee effects or even on their presence and absence. For example, one classical explanation for the appearance of an Allee effect is the difficulty of finding mates. Since there are often differences in movement ability between males and females in a species, different landscape characteristics can change the probability of finding mates and therefore induce (or not) an Allee effect. The ability (or lack thereof) of plants to attract pollinators is another potential mechanism for an Allee effect. Certain landscape features may attract or repulse pollinators locally and therefore affect whether and to what extent plants experience an Allee effect. It is therefore important to consider landscapes in which a population has an Allee effect in some regions but not in others.

In this work, we consider a landscape consisting of two adjacent patches of (possibly) different quality and study the existence and the shape of steady states in such landscapes. In particular, we study the case when the population dynamics have a strong Allee effect on one patch but not the other. In the next section, we formulate our model in detail and provide preliminary information and results on existence of solutions of the resulting system of reaction–diffusion equations. We then show how a positive steady state for our system can be obtained by 'gluing' together solutions of corresponding systems of ordinary differential equations and their solution curves in the phase plane. We obtain a

classification of the shapes of steady states (Section 3). As a consequence, we recover a previous results for steady states when there is no Allee effect, but with different methods. We then study the stability properties of some special steady-state solutions and combine these insights to obtain results on whether and when the system shows bistability, i.e., the existence of multiple stable states (Section 4). It turns out that the relative size of the two patches determines whether there is a global Allee effect if one of the patches shows an Allee effect while the other does not. We use analytical and numerical methods to study some bifurcations in our system (Section 5). We close with a discussion that considers some of the biological implications of our work.

2. Model presentation and preliminaries

We consider a one-dimensional landscape consisting of two adjacent patches. The two patches, say $0 \le x \le l_1$ for patch 1 and $-l_2 \le x \le 0$ for patch 2 with an interface at $x = 0$, can be of different quality, for example, one could represent dense forest while the other is open grassland. We have a population that inhabits this landscape and whose dynamics and movement on each patch are described by a reaction-diffusion equation. Hence, the equation for the population density $u_i(x,t)$ at time t and location x in patch i is

$$\frac{\partial u_i(x,t)}{\partial t} = d_i \frac{\partial^2 u_i(x,t)}{\partial x^2} + h_i(u_i(x,t)), \qquad i = 1,2, \tag{2.1}$$

where d_i represents the diffusion coefficient and h_i describes the net growth. We will consider two types of growth functions:

- Type M: $h(u)$ is a monostable function, that is, there exists a positive number k such that $h(0) = 0 = h(k)$, $h(u) > 0$ if $0 < u < k$ and $h(u) < 0$ if $u > k$. As an example, we have the logistic growth function
$$h(u) = ru\left(1 - \frac{u}{k}\right) \tag{2.2}$$
and the weak Allee function
$$h(u) = ru^2\left(1 - \frac{u}{k}\right). \tag{2.3}$$
- Type B: $h(u)$ is a bistable function, that is, there exist positives numbers a and k, $0 < a < k$, such that $h(0) = h(a) = 0 = h(k)$, $h(u) < 0$ on $(0,a)$, $h(u) > 0$ on (a,k) and $h(u) < 0$ if $u > k$. As an example, we have the following cubic function, which presents a strong Allee effect
$$h(u) = ru\left(\frac{u}{k} - \frac{a}{k}\right)\left(1 - \frac{u}{k}\right). \tag{2.4}$$

We impose no-flux conditions at the boundary points $x = -l_2$ and $x = l_1$, that is

$$\frac{\partial u_2(-l_2,t)}{\partial x} = \frac{\partial u_1(l_1,t)}{\partial x} = 0, \qquad t \ge 0. \tag{2.5}$$

These boundary conditions imply that no individuals are leaving the two-patch landscape.

We consider the following matching conditions at the interface point $x = 0$:

$$u_1(0,t) = \delta u_2(0,t), \qquad t \ge 0, \tag{2.6}$$

$$d_1 \frac{\partial u_1(0,t)}{\partial x} = d_2 \frac{\partial u_2(0,t)}{\partial x}, \qquad t \ge 0, \tag{2.7}$$

where $\delta = \alpha d_2/(1-\alpha)d_1$. Parameter α is the probability that an individual at the interface moves into patch 1 and, accordingly, $1-\alpha$ denotes the probability that the individual moves to patch 2. This expression of parameter δ can be derived from a random walk model [25, 28]. Equation (2.6) says that if individuals have a patch preference ($\alpha \ne 0.5$) and/or unequal movement rates ($d_1 \ne d_2$), then the density is discontinuous at the interface. Equation (2.7) reflects flux conservation at the interface. It

implies that every individual that leaves one patch enters the other and that there is no mortality in this movement across the patch interface.

By assembling equations (2.1), (2.5), (2.6) and (2.7), we obtain the following system of equations to study

$$\begin{cases} \dfrac{\partial u_1(x,t)}{\partial t} = d_1 \dfrac{\partial^2 u_1(x,t)}{\partial x^2} + h_1(u_1(x,t)), & (x,t) \in [0, l_1] \times [0, \infty); \\ \dfrac{\partial u_2(x,t)}{\partial t} = d_2 \dfrac{\partial^2 u_2(x,t)}{\partial x^2} + h_2(u_2(x,t)), & (x,t) \in [-l_2, 0] \times [0, \infty); \\ u_1(0,t) = \delta u_2(0,t), & t \geq 0; \\ d_1 \dfrac{\partial u_1(0,t)}{\partial x} = d_2 \dfrac{\partial u_2(0,t)}{\partial x}, & t \geq 0; \\ \dfrac{\partial u_2(-l_2,t)}{\partial x} = \dfrac{\partial u_1(l_1,t)}{\partial x} = 0, & t \geq 0, \end{cases} \tag{2.8}$$

where each h_i, $i = 1, 2$, can be of type M or B.

The well-posedness of a system very similar to (2.8) has been shown by [24]. We omit the proof of the following result since it requires only minor adjustments to the proofs in their work.

Theorem 2.1. *System (2.8) with nonnegative initial condition $u(x,0) = u_0(x)$ has a unique global solution. Furthermore, if $u_0(x)$ is nonnegative and bounded, then so is the solution.*

To simplify our analysis, we scale system (2.8) such that the density and the derivative at the interface become continuous. As long as $h_2'(0) \neq 0$, we make the following change of variables:

$$\begin{cases} \tau = \beta t, \quad u_1(x,t) = \delta k_2 v_1(\xi, \tau), \quad \xi = x \dfrac{\sqrt{\beta d_2}}{\delta d_1} \in \left[0, l_1 \dfrac{\sqrt{\beta d_2}}{\delta d_1}\right], \\ u_2(x,t) = k_2 v_2(\xi, \tau), \quad \xi = x\sqrt{\beta / d_2} \in \left[-l_2 \sqrt{\beta / d_2}, 0\right], \end{cases} \tag{2.9}$$

where $\beta = h_2'(0)$ if h_2 is of type M or $\beta = -h_2'(0)/ak_2$ if h_2 is of type B.

We obtain the scaled time-dependent problem

$$\begin{cases} \dfrac{\partial v_1(\xi,\tau)}{\partial \tau} = D \dfrac{\partial^2 v_1(\xi,\tau)}{\partial \xi^2} + H_1(v_1(\xi,\tau)), & (\xi,\tau) \in [0, L_1] \times [0, \infty); \\ \dfrac{\partial v_2(\xi,\tau)}{\partial t} = \dfrac{\partial^2 v_2(\xi,\tau)}{\partial x^2} + H_2(v_2(\xi,\tau)), & (\xi,\tau) \in [-L_2, 0] \times [0, \infty); \\ v_1(0,\tau) = v_2(0,\tau), & \tau \geq 0; \\ \dfrac{\partial v_1(0,\tau)}{\partial \xi} = \dfrac{\partial v_2(0,\tau)}{\partial \xi}, & \tau \geq 0; \\ \dfrac{\partial v_2(-L_2,\tau)}{\partial \xi} = \dfrac{\partial v_1(L_1,\tau)}{\partial \xi} = 0, & \tau \geq 0, \end{cases} \tag{2.10}$$

where

$$D = \frac{d_2}{\delta^2 d_1},\ \ L_1 = l_1\frac{\sqrt{\beta d_2}}{\delta d_1},\ \ L_2 = l_2\sqrt{\beta/d_2},\ \ H_1(v_1) = \frac{1}{\beta\delta k_2}h_1(\delta k_2 v_1)\ \text{ and }\ H_2 = \frac{1}{\beta k_2}h_2(k_2 v_2).$$

We notice that H_i is of type M (B) precisely when h_i is.

When $h_2'(0) = 0$, the above scaling with $\beta = 1$ still leads to solutions being continuously differentiable at the interface, but other choices of β (dependent on the specific form of the function) might lead to a greater reduction in the number of remaining parameters.

The steady-state equations of model (2.10) are:

$$\begin{cases} D\dfrac{\mathrm{d}^2 v_1}{\mathrm{d}\xi^2} + H_1(v_1) = 0, & \xi \in [0, L_1]; \\[2ex] \dfrac{\mathrm{d}^2 v_2}{\mathrm{d}\xi^2} + H_2(v_2) = 0, & \xi \in [-L_2, 0]; \\[2ex] v_1(0) = v_2(0),\ \dfrac{\mathrm{d}v_1(0)}{\mathrm{d}\xi} = \dfrac{\mathrm{d}v_2(0)}{\mathrm{d}\xi},\ \dfrac{\mathrm{d}v_2(-L_2)}{\mathrm{d}\xi} = 0,\ \dfrac{\mathrm{d}v_1(L_1)}{\mathrm{d}\xi} = 0. \end{cases} \tag{2.11}$$

We write this system of coupled second-order equations as two systems of coupled first-order equations and use phase-plane methods to analyze solutions (compare [35], [34]). System (2.11) is equivalent to

$$\begin{cases} \begin{cases} \dfrac{\mathrm{d}v_1}{\mathrm{d}\xi} = w_1, \\[2ex] \dfrac{\mathrm{d}w_1}{\mathrm{d}\xi} = -\dfrac{1}{D}H_1(v_1), \end{cases} \quad \Bigg| \quad \begin{cases} \dfrac{\mathrm{d}v_2}{\mathrm{d}\xi} = w_2, \\[2ex] \dfrac{\mathrm{d}w_2}{\mathrm{d}\xi} = -H_2(v_2), \end{cases} \\[2ex] v_1(0) = v_2(0),\ w_1(0) = w_2(0),\ w_2(-L_2) = 0,\ w_1(L_1) = 0. \end{cases} \tag{2.12}$$

It is interesting to note that the ODEs here are coupled only through the interface matching conditions and not through the reaction term. This reflects the spatial structure of the system where individuals in patch 1 interact with individuals in patch 2 only indirectly when crossing the interface.

We analyze system (2.12) for different combinations of population dynamics, i.e., type M or B, which lead to different phase planes of the ODE systems in (2.12). We can have (H_1, H_2) of type (M,M), (M,B) or (B,B) . The case (B,M) is equivalent to the case (M,B) by symmetry. This latter case is the one that we study in this work. Before we study the various combinations of phase-plane dynamics, we give the most important properties of each in isolation, i.e., we study

$$\begin{cases} \dfrac{\mathrm{d}v}{\mathrm{d}\xi} = w, \\[2ex] \dfrac{\mathrm{d}w}{\mathrm{d}\xi} = -H(v). \end{cases} \tag{2.13}$$

The equilibrium points are of the form $(\bar{v}, 0)$ where $H(\bar{v}) = 0$. Their Jacobian matrix has trace zero and determinant equal to $H'(\bar{v})$. Hence, if $H'(\bar{v}) < 0$ then $(\bar{v}, 0)$ is a saddle; if $H'(\bar{v}) > 0$ then $(\bar{v}, 0)$ is a linear centre. The equation has the energy functional (first integral)

$$E(v, w) = \frac{1}{2}w^2 + \int_0^v H(z)\mathrm{d}z. \tag{2.14}$$

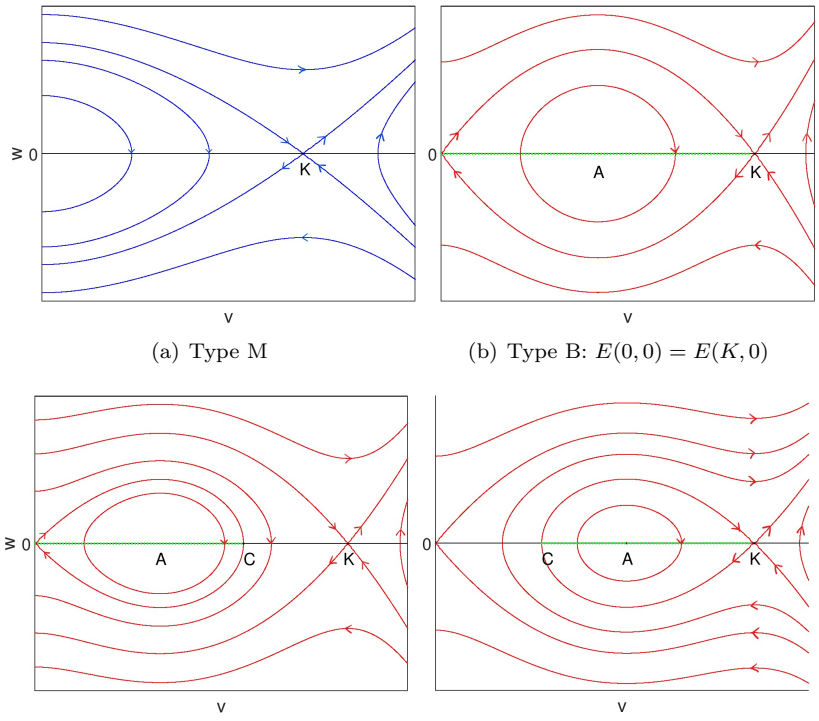

(a) Type M

(b) Type B: $E(0,0) = E(K,0)$

(c) Type B: $E(0,0) < E(K,0)$

(d) Type B: $E(0,0) > E(K,0)$

FIGURE 1. Phase portrait of system (2.13) when H is of type M and of type B. We used functions (2.2) and (2.4) to generate the plots.

Solutions of the ODE system are contained in level sets of E. Using this energy functional, we can show that a linear centre is also a centre for the nonlinear system. In particular, the level sets of E are closed near a linear centre so that the vector field has periodic solutions near such a centre.

When function H is of type M with $H(0) = H(K) = 0$, the qualitative behaviour of solutions of (2.13) is given by the phase plane in Figure 1(a). When function H is of type B with $H(0) = H(A) = H(K) = 0$ and $0 < A < K$, there are three qualitatively different cases. When $E(0,0) = E(K,0)$ then there is a pair of heteroclinic orbits from $(0,0)$ to $(K,0)$ (Figure 1(b)). All nonconstant orbits inside the region bounded by the heteroclinic orbit are periodic. When $E(0,0) < E(K,0)$ then there is a homoclinic orbit from $(0,0)$ (Figure 1(c)). All nonconstant orbits inside the region bounded by the homoclinic orbit are periodic. They intersect the v-axis exactly twice and have the point $(A,0)$ in their interior. When $E(0,0) > E(K,0)$, there is a homoclinic orbit from $(K,0)$ (Figure 1(d)). The remaining properties of the phase plane are as in the preceding case. We denote the point at which a homoclinic intersects the v-axis by $(C,0)$.

Now, we are interested in the periodic orbits inside the homoclinic or heteroclinic. Using (2.14), they satisfy $E(v,w) = c$, which gives

$$w = \pm\sqrt{2\left(c - \int_0^v H(z)\mathrm{d}z\right)}$$

for some $c \in \mathbb{R}$. We denote the intersection of the periodic orbit with the v-axis by ν_1 and ν_2, with $0 < \nu_1 < A < \nu_2 < K$, and the length of the patch by L_p. Integrating over the upper or lower half orbit

yields (compare [23])

$$L_p = \int_{\nu_1}^{\nu_2} \frac{\mathrm{d}v}{\sqrt{2\left(c - \int_0^v H(z)\mathrm{d}z\right)}}. \tag{2.15}$$

For orbits sufficiently close to the center point $(A, 0)$, the length L_p can be approximated by linearizing (2.13) around its equilibrium point $(A, 0)$. We find that $L_p = \pi/\sqrt{H'(A)}$.

3. Shape properties of positive steady states

We begin our analysis of the steady states of (2.10) with several results on their qualitative properties, such as monotonicity and bounds. We obtain these results by analyzing the corresponding systems (2.11) and (2.12). The phase portrait of (2.12) is a combination of Figure 1(a) and one of Figures 1(b), 1(c) and 1(d) depending on the type of function H in each patch (see Figures 2 and 3). For illustration purposes, the phase plane in patch 1 will be represented by blue lines and in patch 2 by red lines. Therefore, a solution of (2.12) consists of a connected orbit that starts on the v-axis on the red vector fields and ends on the v-axis on the blue vector fields. The point where the two orbits meet corresponds to the point at the interface. An obvious and trivial example of such an orbit is the constant solution $(0, 0)$. It corresponds to the extinction of the population in both patches.

3.1. When (H_1, H_2) is of type (M, M).

The constant function $v_1(\xi) = v_2(\xi) = K_1$ is a solution of (2.11) when $K_1 = K_2$. When $K_1 \neq K_2$, the non-constant solutions are characterized by the following result.

Theorem 3.1. *All nonconstant positive solutions of (2.11) (and hence all steady-state solutions of (2.10)) are monotone and bounded between K_1 and K_2.*

Proof. Let $v = (v_1, v_2)$ be a nontrivial positive solution of (2.12) on $[-L_2, L_1]$. Without loss of generality, we may assume that $K_1 > K_2$. If we assume that $v_2(-L_2) < K_2$ then $v_2(\xi) < K_2$ and $w_2(\xi) < 0$ for all $\xi \in (-L_2, 0]$, according to Figure 1(a). Hence, by the interface conditions, we also have $v_1(0) < K_2 < K_1$ and $w_1(0) < 0$. But then, by following the vector field in Figure 1(a) again, we see that $w_1(\xi)$ is decreasing so that the boundary condition $w_1(L_1) = 0$ cannot be met. Hence we require $v_2(-L_2) \geq K_2$. Next, if we assume that $v_2(-L_2) = K_2$ then v_2 and w_2 are constant, so that, by the interface conditions we find $v_1(0) = K_2 < K_1$ and $w_1(0) = 0$. According to the vectorfield, again, we get $w_1(\xi) < 0$ for all $\xi > 0$, so that we cannot satisfy the boundary condition. Hence we must have $v_2(-L_2) > K_2$. By following the vectorfield, we see that the solution is increasing, so that $v_2(0) > K_2$ and $w_2(0) > 0$. A similar argument shows that we must have $v_1(L_1) < K_1$ and that the solution is increasing from $v_1(0)$ to $v_1(L_1)$. Such a solution is indicated in Figure 2. This completes the proof. □

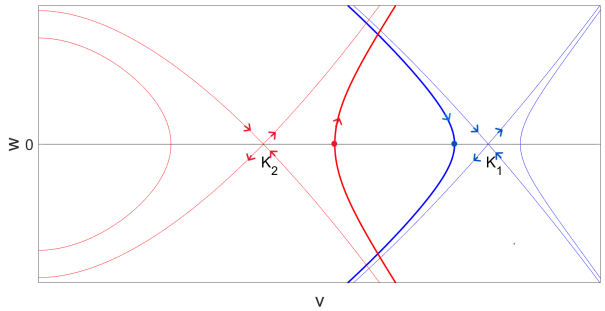

FIGURE 2. Phase portrait of system (2.12) when (H_1, H_2) is of type (M, M) and $K_1 > K_2$. The nonconstant steady state solution of interest is represented by the solution that starts at the red dot, increases to the intersection with the blue solution, then follows that blue solution to the blue dot.

3.2. **When (H_1, H_2) is of type (M, B).** The constant functions $v_1(\xi) = v_2(\xi) = K_1$ are solutions of (2.11) when $K_1 = K_2$ and when $K_1 = A$. Next, we classify all possible and positive nonconstant solutions of systems (2.12) and (2.11), when H_1 is of type M and H_2 of type B, with $K_1 \neq K_2$ and $K_1 \neq A$. First, we reduce the problem of classifying all possible solutions of system (2.12) to the problem of classifying monotone solutions.

Theorem 3.2. (1) *Let $v = (v_1, v_2)$ be a positive nonconstant solution of (2.12) on $[-L_2, L_1]$. Then there exists a length $0 < \bar{L}_2 \leq L_2$ such that the restriction of v to $[-\bar{L}_2, L_1]$ is a monotone solution $v_m = (v_1, v_{2m})$.*

(2) *Let $v_m = (v_1, v_{2m})$ be a monotone solution on $[-L_2, L_1]$. If $(v_m(-L_2), 0)$ is inside the homoclinic or heteroclinic orbit (see Figure 3), then for every integer n, there is a solution $\tilde{v} = (v_1, \tilde{v}_{2m})$ on $[-(L_2 + nL_p), L_1]$, whose restriction to its monotone part is the given solution v_m.*

Proof. Let $v = (v_1, v_2)$ be a solution of (2.12) on $[-L_2, L_1]$. We have shown in Theorem 3.1 that each solution v_1 on patch 1 is monotone. By the interface conditions, this solution comes from patch 2 with the same slope, i.e., $w_2(0) = w_1(0)$ (Recall that we have scaled the system to have continuous density and derivative.) Before it can change slope, the slope has to be zero. When the slope is zero, the boundary condition is satisfied. Hence, there is a length of patch 2 that has this monotone solution. More precisely, we know that $w_2(-L_2) = 0$ by the boundary conditions. If $w_2(\xi) \neq 0$ for all $\xi \in (-L_2, 0)$, then v_2 is monotone since w_2 is the derivative of v_2. If $w_2(\xi) = 0$ for some $\xi \in (-L_2, 0)$, we pick the largest $\bar{\xi} \in (-L_2, 0)$ such that $w_2(\bar{\xi}) = 0$. Then, $v_{2m}(\xi) = v_2(\xi)$ for $\xi \in (\bar{\xi}, 0)$ is monotone. We have proved the first part of the theorem.

Let $v_{2m}(-L_2)$ be inside the homoclinic or heteroclinic orbit. Then there is a periodic orbit through this point and solution v_{2m} oscillates, producing any number n half orbits starting and ending on the v-axis on the distance L_p given by (2.15). Therefore, solutions v_m can be extended on $[-(L_2 + nL_p), L_1]$. We have proved the second part of the theorem.

□

We classify monotone nonconstant solutions of (2.12), and therefore monotone nonconstant steady states of (2.10), in the following theorem.

Theorem 3.3 (Classification of solutions)**.** *Let (v_1, v_2) be a positive monotone solution of (2.12). Generically, this solution is of one of three following types:*

(1) *The solution is strictly increasing in both patches with $v_2(-L_2) < \min\{A, K_1\}$ and $v_1(L_1) < K_1$.*

(2) *The solution is strictly increasing in both patches with* $v_2(-L_2) > K_2$ *and* $v_1(L_1) < K_1$*, provided* $K_1 > K_2$.
(3) *The solution is strictly decreasing in both patches with* $\max\{A, K_1\} < v_2(-L_2) < K_2$ *and* $v_1(L_1) > K_1$*, provided* $K_1 < K_2$.

In addition, the following solutions exist under the accompanying non-generic conditions.

(1) *The solution is strictly increasing on patch 2 with* $v_2(-L_2) < A$ *and constant on patch 1 with* $v_1 \equiv K_1$*, provided that*
   - $K_1 > A$,
   - *The point* $(K_1, 0)$ *is inside the homoclinic or heteroclinic orbit in Figure 3(c) , and*
   - $L_2 = L_p$ *as defined in* (2.15)*, with* $\nu_2 = K_1$.

(2) *The solution is strictly decreasing on patch 2 with* $v_2(-L_2) > A$ *and constant on patch 1 with* $v_1 \equiv K_1$*, provided that*
   - $K_1 < A$,
   - *The point* $(K_1, 0)$ *is inside the homoclinic or heteroclinic orbit in Figure 3(b), and*
   - $L_2 = L_p$ *as defined in* (2.15)*, with* $\nu_1 = K_1$.

Proof. Let $v = (v_1, v_2)$ be a positive monotone nonconstant solution of (2.12). First, we assume that $K_1 < K_2$.

Case 1: We fix $v_2(-L_2) < A$ and assume that $L_2 \neq L_p$. Then following the vector fields in Figure 1(b), the solution is increasing with $w_2(\xi) > 0$ for all $\xi \in (-L_2, 0]$. Hence, by the interface conditions, we also have $w_1(0) > 0$. Then, following the vector fields in Figure 1(a), we see that the boundary condition $w_1(L_1) = 0$ can only be met if $w_1(\xi)$ is decreasing, which implies that $v_1(L_1) < K_1$. Hence, we have $v_2(-L_2) < \min(A, K_1)$ and an increasing solution from $v_1(0)$ to $v_1(L_1)$. Such a solution is present in all the plots in Figures 3(a), 3(b) and 3(d).

Similar arguments can be used to first show that a decreasing solution satisfying $\max(A, K_1) < v_2(-L_2) < K_2$ and $v_1(L_1) > K_1$ exists when $A < v_2(-L_2) < K_2$ and $L_2 \neq L_p$; and second, that there is no solution when $v_2(-L_2) > K_2$ and $L_2 \neq L_p$. Figure 3(b) illustrates a decreasing solution.

Case 2: We fix $K_2 > v_2(-L_2) > A$ and assume that $L_2 = L_p$ with $\nu_2 = v_2(-L_2)$. Then following the vector fields in Figure 1(a), this solution is decreasing with $v_2(0) < A$ and $w_2(0) = 0$. The point $(K_1, 0)$ may be on this orbit if $K_1 < A$. Then we can have $\nu_1 = v_2(0) = K_1$. By the interface conditions, we have $w_1(0) = 0$ and $v_1(0) = K_1$. Since the boundary condition $w_1(L_1) = 0$ is already met at $v_1(0)$, then the solution v_1 is constant and equal to K_1.

Similarly, if we fix $v_2(-L_2) < A$ and assume that $L_2 = L_p$ with $\nu_1 = v_2(-L_2)$, we can find an increasing solution v_2 and a constant solution v_1 if $K_1 > A$ and $\nu_2 = v_2(0) = K_1$. Theses two solutions can be observed in Figures 3(c) and 3(d), respectively.

Second, we assume that $K_1 > K_2$. Then one can use the same arguments as in the proof of Theorem 3.1 to show that there is an increasing solution that is bounded between K_2 and K_1 (see Figure 3(c)). □

In the case (M,M), we have previously shown elsewhere that the positive steady state is unique, and also that it is globally stable among positive solutions; see Theorem 2 in [27]. Since we do not have uniqueness here in general, we cannot expect global stability results. In the next section, we will study local stability properties.

4. Stability properties of positive steady states

In this section, we focus on the case where one patch has monostable and the other bistable dynamics, i.e., (M,B). We consider the eigenvalue problem corresponding to the linearized system of (2.10) at its

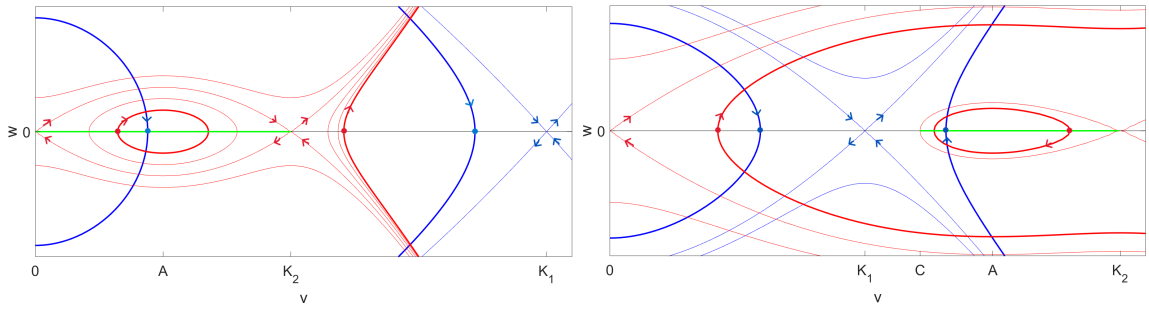

(a) $A < K_2 < K_1$ (b) $K_1 < A < K_2$

(c) $K_1 < A < K_2$ (d) $A < K_1 < K_2$

FIGURE 3. Some phase portraits of system (2.12) when (H_1, H_2) is of type (M,B). As in the previous figure, sample solutions start at a red dot, follow the red vector field until the intersection with the blue vector field, then follow that until the blue dot. Plots c) and d) contain solutions where the red vector field ends at a blue dot; these solutions do not follow the blue vector field for any positive length of time.

steady state solutions, obtain the existence of the principal eigenvalue, and then use the principal eigenvalue to determine the stability of theses steady state solution. We will then use the sub- and supersolutions method to obtain some results on the coexistence of multiple positive steady states. A recent related result by [24] proves the existence of a dominant eigenvalue in the space of continuous functions.

4.1. **The principal eigenvalue and linear stability of a steady state solution.** We linearize the first two equations of (2.10) at a steady state solution, $\bar{v}(\xi) = (\bar{v}_1(\xi), \bar{v}_2(\xi))$, and search for a solution of the form $\eta_i(\xi,\tau) = \exp(\sigma\tau)\psi_i(\xi)$, where $\eta_i(\xi,\tau) = v_i(\xi,\tau) - \bar{v}_i(\xi)$, $i = 1, 2$. The corresponding eigenvalue problem is

$$\mathcal{L}\psi = \sigma\psi \quad \text{where} \quad \mathcal{L} := \begin{pmatrix} D\dfrac{\mathrm{d}^2}{\mathrm{d}\xi^2} + H_1'(\bar{v}_1) & \\ & \dfrac{\mathrm{d}^2}{\mathrm{d}\xi^2} + H_2'(\bar{v}_2) \end{pmatrix} \tag{4.1}$$

with the boundary and interface conditions

$$\psi_1(0) = \psi_2(0),\ \psi_1'(0) = \psi_2'(0),\ \psi_1'(L_1) = 0,\ \psi_2'(-L_2) = 0. \tag{4.2}$$

We set $Y = \left\{(\psi_1, \psi_2) \in W^{2,2}([0, L_1]) \times W^{2,2}([-L_2, 0]) \,|\, \psi \quad \text{satisfies} \quad (4.2)\right\}$. The following result shows that (some of) the classical Sturm-Liouville [1, 13] theory can be generalized to $\mathcal{L}$.

Theorem 4.1. (1) *Each eigenvalue of $\mathcal{L}$ on Y is real.*

(2) *The eigenvalues of $\mathcal{L}$ form an infinite sequence $\{\sigma_k\}_{k=1}^{\infty}$, where*

$$\sigma_1 > \sigma_2 \geq \sigma_3 \geq ... \geq \sigma_k \geq ... \quad with \quad \sigma_k \longrightarrow -\infty \quad as \quad k \longrightarrow \infty.$$

(3) *$\mathcal{L}$ has a principal eigenvalue σ_1 with a positive eigenfunction $\psi = (\psi_1, \psi_2)$ in Y. Moreover, the principal eigenvalue satisfies*

$$\sigma_1 = \max_{\psi \in Y,\, \psi \neq 0} \left\{ \frac{-\int_0^{L_1} (\psi_1')^2 \mathrm{d}\xi - \int_{-L_2}^0 (\psi_2')^2 \mathrm{d}\xi + \frac{1}{D}\int_0^{L_1} H_1'(\bar{v}_1)\psi_1^2 \mathrm{d}\xi + \int_{-L_2}^0 H_2'(\bar{v}_2)\psi_2^2 \mathrm{d}\xi}{\frac{1}{D}\int_0^{L_1} \psi_1^2 \mathrm{d}\xi + \int_{-L_2}^0 \psi_2^2 \mathrm{d}\xi} \right\}. \tag{4.3}$$

We provide the proof of this theorem in Section 6.1. The following proposition gives some properties of the principal eigenvalue (4.3).

Proposition 4.2. *Let $\bar{v} = (\bar{v}_1, \bar{v}_2)$ be a steady state of (2.10). The principal eigenvalue σ_1*

(1) *is negative if $H_1'(\bar{v}_1)$ and $H_2'(\bar{v}_2)$ are both negative. In that case, $\bar{v}$ is linearly stable.*

(2) *is positive if the sum*

$$\int_0^{L_1} H_1'(\bar{v}_1)\mathrm{d}\xi + D\int_{-L_2}^0 H_2'(\bar{v}_2)\mathrm{d}\xi$$

is positive. In that case, $\bar{v}$ is linearly unstable.

(3) *satisfies $\min_\xi(H_1'(\bar{v}_1), H_2'(\bar{v}_2)) \leq \sigma_1 \leq \max_\xi(H_1'(\bar{v}_1), H_2'(\bar{v}_2))$.*

Proof. Let $\bar{v} = (\bar{v}_1, \bar{v}_2)$ be a steady solution of (2.10). If $H_1'(\bar{v}_1)$ and $H_2'(\bar{v}_2)$ are both negative then the numerator of (4.3) is negative. Therefore, $\sigma_1 < 0$ and $\bar{v}$ is stable. In (4.3), the maximum is taken over Y, and constant functions belong to Y, so by taking $\psi = 1$ in (4.3), we obtain

$$\sigma_1 \geq \frac{\int_0^{L_1} H_1'(\bar{v}_1)\mathrm{d}\xi + D\int_{-L_2}^0 H_2'(\bar{v}_2)\mathrm{d}\xi}{L_1 + DL_2} \tag{4.4}$$

Thus,

$$\int_0^{L_1} H_1'(\bar{v}_1)\mathrm{d}\xi + D\int_{-L_2}^0 H_2'(\bar{v}_2)\mathrm{d}\xi > 0$$

implies $\sigma_1 > 0$. Then, $\bar{v}$ is unstable.

Now, we assume that $H_1'(\bar{v}_1)$ and $H_2'(\bar{v}_2)$ depend on ξ. Then, $\min_\xi\{H_1'(\bar{v}_1), H_2'(\bar{v}_2)\} \leq H_i'(\bar{v}_i) \leq \max_\xi\{H_1'(\bar{v}_1), H_2'(\bar{v}_2)\}$. The right-hand side of (4.4) becomes greater than

$$\left(\frac{L_1}{L_1 + DL_2} + \frac{DL_2}{L_1 + DL_2}\right)\min_\xi\{H_1'(\bar{v}_1), H_2'(\bar{v}_2)\}.$$

Therefore, $\sigma_1 \geq \min_\xi(H_1'(\bar{v}_1), H_2'(\bar{v}_2))$. On the other hand, the right-hand side of (4.3) is less than

$$\max_{\psi \in Y,\, \psi \neq 0} \left\{ \frac{\left(\frac{1}{D}\int_0^{L_1} \psi_1^2 \mathrm{d}\xi + \int_{-L_2}^0 \psi_2^2 \mathrm{d}\xi\right)\max_\xi\{H_1'(\bar{v}_1), H_2'(\bar{v}_2)\}}{\frac{1}{D}\int_0^{L_1} \psi_1^2 \mathrm{d}\xi + \int_{-L_2}^0 \psi_2^2 \mathrm{d}\xi} \right\}.$$

Therefore, $\sigma_1 \leq \max_\xi(H_1'(\bar{v}_1), H_2'(\bar{v}_2))$. We conclude that

$$\min_\xi(H_1'(\bar{v}_1), H_2'(\bar{v}_2)) \leq \sigma_1 \leq \max_\xi(H_1'(\bar{v}_1), H_2'(\bar{v}_2)).$$

□

Corollary 4.3. (1) *Suppose* (H_1, H_2) *is of type (M,M) or (M,B) such that* $K_1 = K_2$. *Then the steady state* (K_1, K_2) *is (linearly) stable.*

(2) *The steady state* $(0,0)$ *is unstable when* (H_1, H_2) *is of type (M,M).*

Proof. $H_1'(K_1)$ and $H_2'(K_2)$ are both negative whatever type H_1 and H_2 are. When (H_1, H_2) is of type (M, M), $H_1'(0)$ and $H_2'(0)$ are both positive. Then from Theorem 4.2, (K_1, K_2) is stable and $(0,0)$ is unstable. □

4.2. **Stability properties of steady states** $(0,0)$ **and** (K_1, A), $K_1 = A$**.** We study the stability properties of steady states of system (2.10), namely $(0,0)$ and (K_1, A), with $K_1 = A$, in type (M, B). In type M alone, the zero state is unstable, but in type B alone, it is stable. Hence, we expect that for the combination (M, B), the stability of $(0,0)$ depends on the relative length of the two patch types. If L_2 is large with respect to L_1, then the steady state would be stable, otherwise unstable. We can explicitly calculate the boundary of L_2 where the stability switches. A similar effect was first observed in an infinite periodic model [30]. The reverse consideration applies to (K_1, A): the constant state K_1 is stable on type M alone and the constant state A is unstable on type B alone.

After lengthy but standard calculations (see [25]), we find that the boundaries of the stability region depend on model parameters as follows:

$$\text{For } (0,0): \bar{L}_2 = \frac{1}{\sqrt{-H_2'(0)}} \operatorname{arctanh}\left[\sqrt{\frac{H_1'(0)}{-DH_2'(0)}} \tan\left(\sqrt{\frac{H_1'(0)}{D}} L_1\right)\right]. \tag{4.5}$$

$$\text{For } (K_1, A): \bar{L}_2 = \frac{1}{\sqrt{H_2'(A)}} \arctan\left[\sqrt{\frac{-H_1'(K_1)}{DH_2'(A)}} \tanh\left(\sqrt{\frac{-H_1'(K_1)}{D}} L_1\right)\right]. \tag{4.6}$$

Note that $-H_2'(0) > 0$ and $-H_1'(K_1) > 0$. Hence, we have the following result:

Theorem 4.4. (1) *Define* $\bar{L}_2$ *as in* (4.5). *Then* $(0,0)$ *is a locally asymptotically stable state of (2.10) if* $L_2 \geq \bar{L}_2$ *and unstable if* $L_2 < \bar{L}_2$.

(2) *Define* $\bar{L}_2$ *as in* (4.6). *Then* (K_1, A) *is a locally asymptotically stable state of (2.10) if* $L_2 \leq \bar{L}_2$ *and unstable if* $L_2 > \bar{L}_2$.

We illustrate the stability region of these two solutions in the L_1–L_2 plane and identify possible regions of bistability with respect to these parameters. In (4.5), the boundary value L_2 in an increasing function of $H_1'(0)$ and L_1, and a decreasing function of $-H_2'(0)$ and D. We find a vertical asymptote for L_2 at

$$L = L_1^c \equiv \sqrt{D/H_1'(0)} \arctan\sqrt{-DH_2'(0)/H_1'(0)}.$$

In (4.6), the boundary value L_2 is an increasing function of $-H_1'(K_1)$ and L_1, and a decreasing function of $H_2'(A)$ and D. Moreover, as L_1 increases, this boundary curve approaches a horizontal asymptote $L_2 = L_2^c$, where

$$L_2^c \equiv \sqrt{1/H_2'(A)} \arctan\sqrt{-H_1'(K_1)/DH_2'(A)}.$$

We find the derivatives of (4.5) and (4.6) at zero because comparison of the two will give us the region of instability and bistability. At the state $(0,0)$, we have $L_2'(0) = -H_1'(0)/DH_2'(0)$ and at (K_1, A), $L_2'(0) = -H_1'(K_1)/DH_2'(A)$.

To illustrate, we use the functions (2.2) and (2.4) in which case $H_1'(0) = R$, $H_2'(0) = -A$, $H_1'(K_1) = -R$ and $H_2'(A) = A(1-A)$. Notice that $H_1'(K_1)$ does not depend on K_1 but $H_2'(A)$ does depend on A. Equations (4.5) and (4.6), with their derivatives at $L_1 = 0$ become

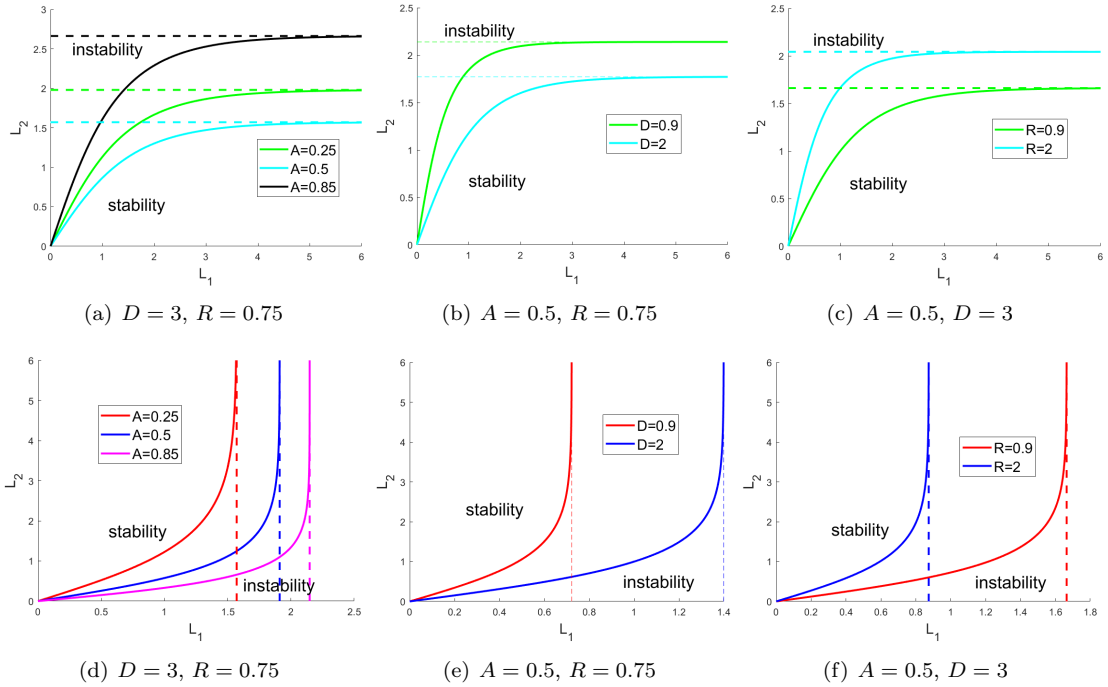

(a) $D = 3$, $R = 0.75$ (b) $A = 0.5$, $R = 0.75$ (c) $A = 0.5$, $D = 3$

(d) $D = 3$, $R = 0.75$ (e) $A = 0.5$, $R = 0.75$ (f) $A = 0.5$, $D = 3$

FIGURE 4. Boundaries (4.5) and (4.6) of the stability regions as a function of patch sizes L_1 and L_2. Panels (a)-(c): at the state (K_1, A). Panels (d)-(f): at the state $(0, 0)$. The dashed lines represent the asymptotes.

$$\text{For } (0,0): L_2 = \frac{1}{\sqrt{A}}\operatorname{arctanh}\left[\sqrt{\frac{R}{AD}}\tan\left(\sqrt{\frac{R}{D}}L_1\right)\right], L_2'(0) = \frac{R}{AD}. \tag{4.7}$$

$$\text{For } (K_1,A): L_2 = \frac{1}{\sqrt{A(1-A)}}\arctan\left[\sqrt{\frac{R}{A(1-A)D}}\tanh\left(\sqrt{\frac{R}{D}}L_1\right)\right], L_2'(0) = \frac{R}{A(1-A)D}. \tag{4.8}$$

For both steady states, the stability region is presented in Figure 4. We plot L_2 as a function of L_1, first, with fixed values of D and R for different values of A; second, with fixed values of A and R for different values of D; third, with fixed value of A and D for different values of R. For these three plots, $(0, 0)$ is stable above the boundary curve (see Figure 4(d), (e) and (f)), while (K_1, A) is stable below the boundary curve (see Figure 4(a), (b) and (c)).

We are now interested in the combination of the plots in Figure 4. Looking at (4.7) and (4.8), since $0 < A < 1$, the slope $L_2'(0)$ for the state $(0, 0)$ is less than that for (K_1, A). We then conclude that the stability domain of the solution (K_1, A) is above the one of $(0, 0)$ for small L_1 and below for large L_1, so that both domains intersect. Figure 5 presents the combination of plots in Figures 4(a) and 4(d). We obtain four different regions. In region (I), the state $(0, 0)$ is stable and the state (K_1, A) is unstable whereas the stability is reversed in region (III). The states $(0, 0)$ and (K_1, A) are both unstable in region (II), while they are both stable in region (IV).

We analyze the regions where at least one of the states $(0, 0)$ and (K_1, A) is unstable. We use sub- and supersolutions methods to show the existence of multiple positive stable steady state solution of system (2.10). We have the following result:

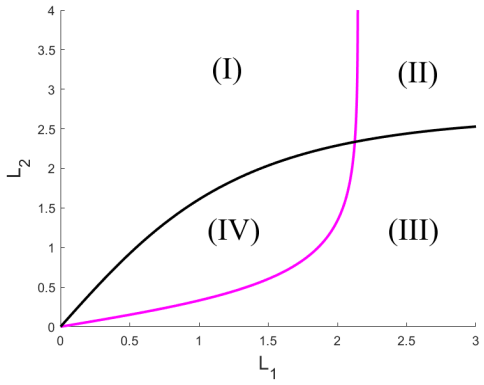

FIGURE 5. Stability regions of steady state $(0,0)$ and (K_1, A). I: only $(0,0)$ is stable, II: both are unstable, III: only (K_1, A) is stable and IV: both are stable. Parameter values are $A = 0.85$, $R = 0.75$ and $D = 3$.

Theorem 4.5. (1) *In region I, system (2.10) has at least one nonconstant stable positive steady state.*

(2) *In region II, system (2.10) has at least two nonconstant stable positive steady states.*

Proof. We apply the idea developed in [6], Section 3.2. Consider the eigenvalue problem (4.1)–(4.2) at $(\bar{v}_1(\xi), \bar{v}_2(\xi)) = (0,0)$ and $(\bar{v}_1(\xi), \bar{v}_2(\xi)) = (K_1, A)$, with respective principal eigenvalues σ_1^0 and σ_1^1, and let $\psi_0 = (\psi_{01}, \psi_{02})$ and $\psi_1 = (\psi_{11}, \psi_{12})$ be the corresponding positive eigenfunctions. When the states $(0,0)$ and (K_1, A) are unstable, then $\sigma_1^0 > 0$ and $\sigma_1^1 > 0$. We construct sub- and supersolutions as appropriate multiples of ψ_0 and ψ_1. The assumptions on H_i imply that, if z is small, we can write $H_i(\bar{v}_i + z) = H_i(\bar{v}_i) + H_i'(\bar{v}_i)z + G_i(\bar{v}_i, z)z^2$, where G_i is a C^2 function in v_i. For ϵ sufficiently small, we set: $(v_{11}, v_{12}) = (\epsilon\psi_{01}, \epsilon\psi_{02})$, $(v_{21}, v_{22}) = (K_1 + \epsilon\psi_{11}, A + \epsilon\psi_{12})$, $(v_{31}, v_{32}) = (K_1 - \epsilon\psi_{11}, A - \epsilon\psi_{12})$ and $(v_{41}, v_{42}) = (K, K)$, where $K \geq K_2$ is a positive constant. We have that:

$$\begin{cases} D\dfrac{\mathrm{d}^2 v_{21}}{\mathrm{d}\xi^2} + H_1(v_{21}) = \epsilon\psi_{11}\left(\sigma_1^1 + G_1(A, \epsilon\psi_{11})\epsilon\psi_{11}\right) > 0, \\ \dfrac{\mathrm{d}^2 v_{22}}{\mathrm{d}\xi^2} + H_2(v_{22}) = \epsilon\psi_{12}\left(\sigma_1^1 + G_2(A, \epsilon\psi_{12})\epsilon\psi_{12}\right) > 0, \\ v_{21}(0) - v_{22}(0) = 0, \ \dfrac{\mathrm{d}v_{21}(0)}{\mathrm{d}\xi} - \dfrac{\mathrm{d}v_{21}(0)}{\mathrm{d}\xi} = 0, \ \dfrac{\mathrm{d}v_{22}(-L_2)}{\mathrm{d}\xi} = 0, \ \dfrac{\mathrm{d}v_{21}(L_1)}{\mathrm{d}\xi} = 0. \end{cases}$$

Hence, (v_{21}, v_{22}) satisfy the definition of a subsolution of the equilibrium problem (2.11). A supersolution of (2.11) will satisfy the reverse inequalities. Similarly, we can show that (v_{11}, v_{12}) is a subsolution for (2.11), (v_{31}, v_{32}) and (v_{41}, v_{42}) are both supersolutions for (2.11).

In region II, $(0,0)$ and (K_1, A) are both unstable. We consider two cases.

Case 1: If $\underline{v}(\xi, \tau)$ is a solution of (2.10) with $\underline{v}(\xi, 0) = (v_{11}, v_{12})$, then $\underline{v}(\xi, \tau)$ is an increasing solution in τ. If $\overline{v}(\xi, \tau)$ is a solution of (2.10) with $\overline{v}(\xi, \tau) = (v_{31}, v_{32})$, then $\overline{v}(\xi, \tau)$ is decreasing in τ. Since, $0 < v_{11} < v_{31} < K_1$ and $0 < v_{12} < v_{32} < A$, then by monotonicity $(0,0) < \underline{v}(\xi, \tau) < \overline{v}(\xi, \tau) < (K_1, A)$. Hence, there exists a positive steady state (v_1^0, v_2^0) of (2.10) satisfying $v_{11} < v_1^0 < v_{31}$ and $v_{12} < v_2^0 < v_{32}$.

Case 2: If $\underline{v}(\xi, \tau)$ is a solution of (2.10) with $\underline{v}(\xi, 0) = (v_{21}, v_{22})$, then $\underline{v}(\xi, \tau)$ is an increasing solution in τ. If $\overline{v}(\xi, \tau)$ is a solution of (2.10) with $\overline{v}(\xi, \tau) = (v_{41}, v_{42})$, then $\overline{v}(\xi, \tau)$ is decreasing in τ. Since for small ϵ, $K_1 + \epsilon\psi_{11} < K_2$ and $A + \epsilon\psi_{12} < K_2$, then by monotonicity $\underline{v}(\xi, \tau) <$

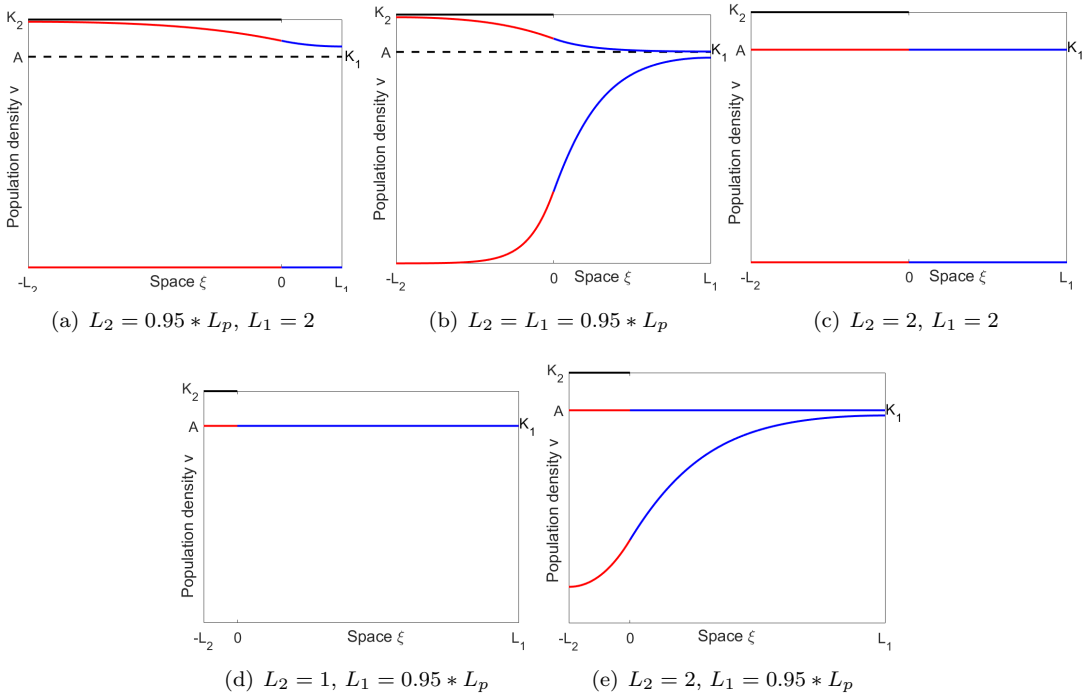

(a) $L_2 = 0.95 * L_p$, $L_1 = 2$ (b) $L_2 = L_1 = 0.95 * L_p$ (c) $L_2 = 2$, $L_1 = 2$

(d) $L_2 = 1$, $L_1 = 0.95 * L_p$ (e) $L_2 = 2$, $L_1 = 0.95 * L_p$

FIGURE 6. Different shapes of steady states corresponding to different regions in Figure 5. The blue (red) parts of the curves correspond to the solution in patch 1 (patch 2); the dashed lines correspond to solution (K_1, A) when it is unstable. The black line at K_2 on patch 2 only serves to visually indicate the carrying capacity there and is not part of a solution. We used the logistic growth function on patch 1 and the Allee growth function on patch 2. Parameters are $A = 0.85$, $R = 0.75$, $D = 3$, and $L_p = 8.7982$.

$\overline{v}(\xi, \tau)$. Hence, there exists a positive steady state (v_1^1, v_2^1) of (2.10) satisfying $v_{21} < v_1^1 < v_{41}$ and $v_{22} < v_2^1 < v_{42}$.

Therefore, when $(0, 0)$ and (K_1, A) are both unstable, at least two nonconstant bounded positive stable solution exist in region II.

In region I, the state $(0, 0)$ is stable and (K_1, A) is unstable. The same arguments as in Case 2 above show the existence of a nonconstant positive stable steady state here. □

Remark 4.1. In region III, the system (2.10) may or may not have a nonconstant stable positive steady state (see Figure 6 below).

Figure 6 shows the different steady states of (2.10) according to the four regions of stability of the constant solutions $(0, 0)$ and (K_1, A) obtained in Figure 5. In region I, in addition to the zero steady state, we have a decreasing solution between K_1 and K_2 (Figure 6(a)). As we increase L_1, we move into region II, so that the zero state loses stability and an increasing solution appears. We now have two positive nonconstant steady states (Figure 6(b)). Alternatively, in region IV, both constant steady states are stable and we do not observe any nonconstant steady states (Figure 6(c)). Finally, in region III, there may or may not be a nonconstant stable steady state; see Figures 6(d) and 6(e).

Since the black and pink curves in Figure 5 correspond to a real dominant eigenvalue crossing zero, and given the shapes of steady states found in Figure 6, it seems reasonable to expect that both curves correspond to transcritical bifurcations. Specifically, the pink curve appears to correspond to a transcritical bifurcation where the trivial state $(0,0)$ is stable on the left (Figures 6(a) and 6(c)) and unstable on the right (Figures 6(b) and 6(e)). Similarly, the black curve appears to correspond to a transcritical bifurcation where the intermediate state (K_1, A) is stable below (Figures 6(c) and 6(e)) and unstable above (Figures 6(a) and 6(b)). We explore these bifurcations more closely in the following section. The situation in Figure 6(d), which can only occur inside region III, requires a different bifurcation, which we will illustrate numerically in the following section.

All the results above hold for the special case that $K_1 = A$, but they can also give us information on the case when K_1 is close but not equal to A.

Lemma 4.6. *If the constant steady state for $K_1 = A$ of (2.10) is linearly stable, then there is a nonconstant steady state when K_1 is close enough but not equal to A.*

The proof of this lemma is an application of the implicit function theorem; see e.g., Chapter 3 in [6]. We omit it here, but the reader can find details in Lemma 4.3.7, Section 4.3 in [18].

5. Bifurcation

In this section, we consider in more detail the behavior of our system when one of the spatially constant states becomes unstable at the values of L_2 that we calculated explicitly in the preceding section. Specifically, we show the bifurcation of some non-constant steady-state solutions of (2.10), following [10] and using the length of patch 2, L_2, as bifurcation parameter.

Rather than having the bifurcation parameter in our spatial domain, we would like to fix the domain and bring the bifurcation parameter into the equations. We can achieve this by scaling the coordinates in each patch by their respective length (on patch i, $\xi = L_i\tilde{\xi}$ and $\mathrm{d}v_i/\mathrm{d}\tilde{\xi} = L_i \mathrm{d}v_i/\mathrm{d}\xi$). Then the steady state equations of system (2.10), given by (2.11), can be rewritten as

$$\begin{cases} D\dfrac{\mathrm{d}^2 v_1}{\mathrm{d}\xi^2} + L_1^2 H_1(v_1) = 0, & \tilde{\xi} \in [0,1]; \\[2ex] \dfrac{\mathrm{d}^2 v_2}{\mathrm{d}\xi^2} + L_2^2 H_2(v_2) = 0, & \tilde{\xi} \in [-1,0]; \\[2ex] v_1(0) = v_2(0), \ \dfrac{\mathrm{d}v_2(0)}{\mathrm{d}\xi} = \dfrac{L_2}{L_1}\dfrac{\mathrm{d}v_1(0)}{\mathrm{d}\xi}, \ \dfrac{\mathrm{d}v_2(-1)}{\mathrm{d}\xi} = 0, \ \dfrac{\mathrm{d}v_1(1)}{\mathrm{d}\xi} = 0. \end{cases} \tag{5.1}$$

We consider the bifurcation of a nontrivial solution of (2.10) from the zero steady state solution at some bifurcation point $L_2 = \bar{L}_2$, defined in (4.7).

Theorem 5.1. *Let $\sigma_1 = \sigma_1(L_2)$ be the principal eigenvalue of the linearization of (5.1) at zero and denote by (ψ_1, ψ_2) the positive eigenfunction associated with $L_2 = \bar{L}_2$, where $\sigma_1(\bar{L}_2) = 0$. Then the following hold.*

1. *$L_2 = \bar{L}_2$ is a bifurcation point for (5.1).*
2. *Near $\big(\bar{L}_2, (0,0)\big)$, the set Γ of positive solutions of (5.1) bifurcating from the line of constant solutions $\{(L_2, (0,0)) : L_2 > 0\}$ has the form:*

$$\Gamma = \{(L_2(s), (v_1(s), v_2(s)) : -\delta < s < \delta\},$$

where δ is a positive constant and $(v_1(s), v_2(s)) = (s\psi_1 + sz_1(s), s\psi_2 + sz_2(s))$ with differentiable functions $L_2(s)$, $z(s) = (z_1(s), z_2(s))$ satisfying $L_2(0) = \bar{L}_2$, and $z(0) = z'(0) = (0,0)$.

(3) *There exists a length L_1^* such that for $L_1 < L_1^*$, the bifurcation is backward and for $L_1 > L_1^*$, the bifurcation is forward.*

The proof of this theorem is given in Section 6.2.

We illustrate the statement of this theorem in Figure 7 below. We plot the value of $v_1(0) = v_2(0)$ of a steady-state solution as a function of L_2. For $v_1(0) = 0$ and $v_1(0) = A = K_1$, we indicate the stability as calculated in Section 4, where a solid (dashed) line indicates a stable (unstable) solution. When L_1 is small, the bifurcation from $(0, 0)$ is backward, which means that the stable branch has negative values. Since this is biologically irrelevant, we do not plot it here (Figure 7(a)). When L_1 is large enough, the bifurcation is forward, which means that the stable branch is positive here (as indicated in Figures 7(b) and 7(c)). When L_1 is intermediate, then the bifurcation value $\bar{L}_2$ is finite (near $L_2 = 2$ in Figure 7(b)). When L_1 is so large that patch 1 alone can support a population, then the zero state is unstable, independent of the value of L_1 (Figure 7(c)).

The same theory can be applied to study the bifurcation behavior at the positive state (K_1, A). The numerical results, included in Figure 7, indicate that the bifurcation from that state is always forward. Looking at Figure 7, we expect branches of unstable solutions. In Figure 7(a), the branch would connect the backward transcritical bifurcation from $(0, 0)$ to the bifurcation point on (K_1, A), In Figures 7(b) and 7(c), we expect the branch to connect the left endpoint of curve of nonconstant stable solutions to the bifurcation point from (K_1, A). In other words, we expect that the endpoints indicate a saddle-node bifurcation. Saddle-node bifurcations are common in connection with a strong Allee effects.

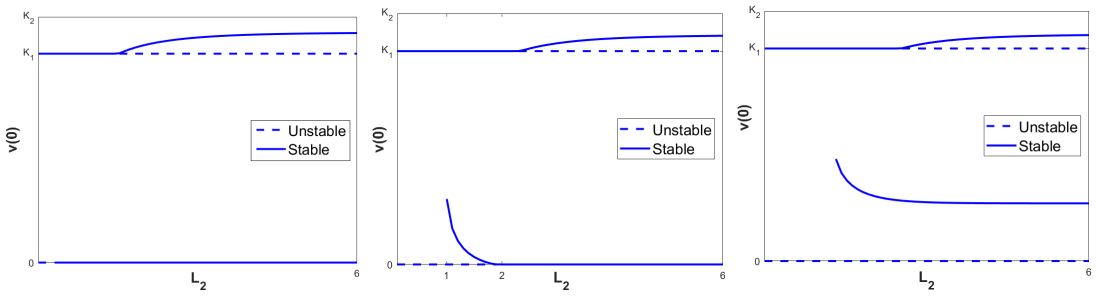

(a) $L_1 = 1$ (b) $L_1 = 2.13$ (c) $L_1 = 3.5$

FIGURE 7. Bifurcation diagram with respect to L_2. Parameters are $K_1 = A = 0.85$, $R = 0.75$, $D = 3$. We used the logistic growth function in patch 1 and the Allee growth function in patch 2.

6. Proofs

6.1. **Proof of Theorem 4.1.** The method used to prove this theorem is an adaptation of the one used to prove related theorems in [6] and [4]. We only indicate the main steps here; more details can be found in [18].

We consider the separable Hilbert space $H = L^2([0, L_1]) \times L^2([-L_2, 0])$ as our base space. On H, we define the inner product

$$(\psi, \phi)_H = \frac{1}{D} \int_0^{L_1} \psi_1 \phi_1 \mathrm{d}\xi + \int_{-L_2}^{0} \psi_2 \phi_2 \mathrm{d}\xi$$

and obtain the norm

$$\|\psi\|_H^2 = \frac{1}{D} \|\psi_1\|_{L^2([0,L_1])}^2 + \|\psi_2\|_{L^2([-L_2,0])}^2.$$

We set $Y := \left\{(\psi_1, \psi_2) \in W^{2,2}([0, L_1]) \times W^{2,2}([-L_2, 0]) \mid \psi \quad \text{satisfies} \quad (4.2)\right\}$ and define the operator

$$-\mathcal{L} := \begin{pmatrix} -D\dfrac{\mathrm{d}^2}{\mathrm{d}\xi^2} + c_1 & \\ & -\dfrac{\mathrm{d}^2}{\mathrm{d}\xi^2} + c_2 \end{pmatrix}.$$

We assume that c_i are positive continuous functions and denote by $\alpha_i := \min c_i$ and $\beta_i = \|c_i\|_\infty$. For brevity, we will denote derivatives with respect to ξ by primes.

Step 1: We multiply $-\mathcal{L}\psi = \sigma\psi$ by a function $\phi = (\phi_1, \phi_2) \in Y$ and integrate to find the bilinear form $B[\cdot, \cdot]$ associated with the elliptic operator $-\mathcal{L}$ as

$$B[\psi, \phi] = \int_0^{L_1} \psi_1'\phi_1' \mathrm{d}\xi + \int_{-L_2}^0 \psi_2'\phi_2' \mathrm{d}\xi + \frac{1}{D}\int_0^{L_1} c_1\psi_1\phi_1 \mathrm{d}\xi + \int_{-L_2}^0 c_2\psi_2\phi_2 \mathrm{d}\xi \tag{6.1}$$

for $\psi, \phi \in X$, where $X = \left\{(\psi_1, \psi_2) \in W^{1,2}([0, L_1]) \times W^{1,2}([-L_2, 0])\right\}$. This bilinear form defines an inner product $(\psi, \phi)_B := B[\psi, \phi]$ on X.

Step 2: We also define the inner product

$$(\psi, \phi)_X = \frac{1}{D}\int_0^{L_1} (\psi_1\phi_1 + \psi_1'\phi_1') \,\mathrm{d}\xi + \int_{-L_2}^0 (\psi_2\phi_2 + \psi_2'\phi_2') \,\mathrm{d}\xi,$$

from which we obtain the norm

$$\|\psi\|_X^2 = \frac{1}{D}\left(\|\psi_1\|^2_{L^2([0,L_1])} + \|\psi_1'\|^2_{L^2([0,L_1])}\right) + \left(\|\psi_2\|^2_{L^2([-L_2,0])} + \|\psi_2'\|^2_{L^2([-L_2,0])}\right).$$

For brevity, we will use the index L^2 instead of $L^2([-L_2, 0])$ or $L^2([0, L_1])$ if no confusion can arise. We can show by standard estimates that the two inner products $(\psi, \phi)_B$ and $(\psi, \phi)_X$ generate equivalent norms.

Step 3: For any fixed $\psi \in X$, we define the linear functional

$$G(\psi) : \phi \mapsto \frac{1}{D}\int_0^{L_1} \psi_1\phi_1 \mathrm{d}\xi + \int_{-L_2}^0 \psi_2\phi_2 \mathrm{d}\xi.$$

It is not too hard to show that G is bounded. Hence, the Riesz Representation theorem (eg [13]) implies that there exists a unique $\varphi := T\psi \in X$ such that $(T\psi, \phi)_B = G(\psi)\phi$, where T is an operator defined on X. We show that T is a positive compact symmetric operator on X.

Since $G(\psi)\phi = G(\phi)\psi$ and $G(\psi)$ is bounded, T is symmetric and bounded. Furthermore, $(T\psi, \psi)_B = G(\psi)\psi = \|\psi\|_H^2 \geq 0$. Thus, T is positive. Let show that T is compact. We consider a bounded sequence $\{\psi_k\}_{k=1}^\infty$ in X. Since X is a Hilbert space, the sequence $\{\psi_k\}_{k=1}^\infty$ has a weakly convergent subsequence $\{\psi_{k_j}\}_{j=1}^\infty$, that is, there exists $\psi \in X$ such that $(\psi_{k_j}, \phi)_X \to (\psi, \phi)_X$ as $j \to \infty$ for all $\phi \in X$ (see [15], Theorem 5.12). The compact embedding of $W^{1,2}$ in L^2 implies $\psi_{k_j} \to \psi$ as $j \to \infty$ in H. We have that:

$$\begin{aligned}
\|T\psi_{k_j} - T\psi\|_B^2 &= \left(T(\psi_{k_j} - \psi), T\psi_{k_j} - T\psi\right)_B \\
&= \frac{1}{D}\int_0^{L_1} (\psi_{k_j} - \psi)_1 \left(T\psi_{k_j} - T\psi\right)_1 \mathrm{d}\xi + \int_{-L_2}^0 (\psi_{k_j} - \psi)_2 \left(T\psi_{k_j} - T\psi\right)_2 \mathrm{d}\xi \\
&\leq C_2 \left\|\psi_{k_j} - \psi\right\|_H \left\|T\psi_{k_j} - T\psi\right\|_B.
\end{aligned}$$

Thereby, $\|T\psi_{k_j} - T\psi\|_B \leq C_2 \left\|\psi_{k_j} - \psi\right\|_H$. Therefore, $\{T\psi_{k_j}\}_{j=1}^{\infty}$ converges in X. We then conclude that T is compact.

Step 4: From the properties of T, we conclude that there exists a countable orthonormal basis $\{\varphi_k\}_{k=1}^{\infty}$ of X, consisting of eigenvectors of T, that each eigenvalue of T is real, and that the eigenvalues form a discrete sequence $\{\mu_k\}_{k=1}^{\infty}$ tending to zero as k goes to infinity [13, 1].

For $\mu_k \neq 0$, we take the inner product of $T\varphi_k = \mu_k\varphi_k$ with any $\phi \in X$ to get $(T\varphi_k, \phi)_B = \mu_k(\varphi_k, \phi)_B$. By the definition of T and the inner product $(\cdot,\cdot)_B$, we get $G(\varphi_k)\phi = \mu_k B[\varphi_k, \phi]$. After dividing by μ_k, this becomes

$$\begin{aligned}&\frac{1}{\mu_k}\left(\frac{1}{D}\int_0^{L_1}\varphi_{k_1}\phi_1 \mathrm{d}\xi + \int_{-L_2}^{0}\varphi_{k_2}\phi_2 \mathrm{d}\xi\right)\\ &= \int_0^{L_1}\varphi'_{k_1}\phi'_1 \mathrm{d}\xi + \int_{-L_2}^{0}\varphi'_{k_2}\phi'_2 \mathrm{d}\xi + \frac{1}{D}\int_0^{L_1} c_1\varphi_{k_1}\phi_1 \mathrm{d}\xi + \int_{-L_2}^{0} c_2\varphi_{k_2}\phi_2 \mathrm{d}\xi.\end{aligned}$$

Since this holds for all ϕ in X, φ_k is a weak solution to

$$\begin{cases} -D\dfrac{\mathrm{d}^2 v_1}{\mathrm{d}\xi^2} + c_1 v_1 = \dfrac{1}{\mu_k} v_1, & \xi \in [0, L_1];\\[2ex] -\dfrac{\mathrm{d}^2 v_2}{\mathrm{d}\xi^2} + c_2 v_2 = \dfrac{1}{\mu_k} v_2, & \xi \in [-L_2, 0];\\[2ex] v_1(0) = v_2(0),\ \dfrac{\mathrm{d}v_2(0)}{\mathrm{d}\xi} = \dfrac{\mathrm{d}v_1(0)}{\mathrm{d}\xi},\ \dfrac{\mathrm{d}v_2(-L_2)}{\mathrm{d}\xi} = 0,\ \dfrac{\mathrm{d}v_1(L_1)}{\mathrm{d}\xi} = 0. \end{cases}$$

By standard elliptic regularity theory, φ_k will belong to Y. Thus, the eigenvalues of $-\mathcal{L}$ are the sequence $\{\lambda_k\}_{k=1}^{\infty}$, where $\lambda_k = \dfrac{1}{\mu_k}$ satisfies $\lambda_1 \leq \lambda_2 \leq \lambda_3 \leq ...$ and $\lambda_k \to \infty$ as $k \to \infty$. It then follows that the eigenvalues of the operator $\mathcal{L}$ are the discrete sequence $\{\sigma_k\}_{k=1}^{\infty}$, where $\sigma_k = -\lambda_k$ satisfy $\sigma_1 > \sigma_2 \geq \sigma_3 \geq ... \geq \sigma_k \geq ...$ with $\sigma_k \to -\infty$ as $k \to \infty$. The principal eigenvalue of $\mathcal{L}$ is given by [13]

$$\sigma_1 = \max_{\psi \in X,\, \psi \neq 0}\left\{\frac{-\displaystyle\int_0^{L_1}(\psi'_1)^2 \mathrm{d}\xi - \int_{-L_2}^{0}(\psi'_2)^2 \mathrm{d}\xi - \frac{1}{D}\int_0^{L_1} c_1\psi_1^2 \mathrm{d}\xi - \int_{-L_2}^{0} c_2\psi_2^2 \mathrm{d}\xi}{\dfrac{1}{D}\displaystyle\int_0^{L_1}\psi_1^2 \mathrm{d}\xi + \int_{-L_2}^{0}\psi_2^2 \mathrm{d}\xi}\right\}.$$

Positivity of the eigenfunction φ_1 was shown in [24]; see also [4] for a more general method.

As in [24], if c_i are not positive, we pick a large enough constant $q > 0$ and solve instead the problem

$$\begin{cases} -D\dfrac{\mathrm{d}^2 v_1}{\mathrm{d}\xi^2} + (c_1 + q)v_1 = (\lambda + q)v_1 = \tilde{\lambda} v_1, & \xi \in [0, L_1];\\[2ex] -\dfrac{\mathrm{d}^2 v_2}{\mathrm{d}\xi^2} + (c_2 + q)v_2 = (\lambda + q)v_2 = \tilde{\lambda} v_2, & \xi \in [-L_2, 0];\\[2ex] v_1(0) = v_2(0),\ \dfrac{\mathrm{d}v_2(0)}{\mathrm{d}\xi} = \dfrac{\mathrm{d}v_1(0)}{\mathrm{d}\xi},\ \dfrac{\mathrm{d}v_2(-L_2)}{\mathrm{d}\xi} = 0,\ \dfrac{\mathrm{d}v_1(L_1)}{\mathrm{d}\xi} = 0. \end{cases}$$

When $c_i + q > 0$, the previous reasoning applies, and eigenvalues $\tilde{\sigma}_1 = -\tilde{\lambda}_1$ exist, but the principal eigenvalues $\sigma_1 = \tilde{\sigma}_1 + q$ need not be negative. Due to this insight, we can use $c_i = H_i'(\bar{v}_i)$ in the formula

above and obtain the desired expression for the dominant eigenvalue

$$\sigma_1 = \max_{\psi\in X,\,\psi\neq 0}\left\{\frac{-\int_0^{L_1}(\psi_1')^2\mathrm{d}\xi-\int_{-L_2}^{0}(\psi_2')^2\mathrm{d}\xi+\frac{1}{D}\int_0^{L_1}H_1'(\bar v_1)\psi_1^2\mathrm{d}\xi+\int_{-L_2}^{0}H_2'(\bar v_2)\psi_2^2\mathrm{d}\xi}{\frac{1}{D}\int_0^{L_1}\psi_1^2\mathrm{d}\xi+\int_{-L_2}^{0}\psi_2^2\mathrm{d}\xi}\right\}. \tag{6.2}$$

6.2. **Proof of Theorem 5.1.** We define $X = L^2([-1,0])\times L^2([0,1])$, $W = W^{2,2}([-1,0])\times W^{2,2}([0,1])$ and a nonlinear mapping $F:\mathbb{R}\times W\to X\times\mathbb{R}^4$ as

$$F(L_2,(v_1,v_2)) = \begin{pmatrix} D\dfrac{\mathrm{d}^2v_1}{\mathrm{d}\xi^2}+L_1^2H_1(v_1)\\[2ex] \dfrac{\mathrm{d}^2v_2}{\mathrm{d}\xi^2}+L_2^2H_2(v_2)\\[2ex] v_1(0)-v_2(0)\\[2ex] \dfrac{\mathrm{d}v_2(0)}{\mathrm{d}\xi}-\dfrac{L_2}{L_1}\dfrac{\mathrm{d}v_1(0)}{\mathrm{d}\xi}\\[2ex] \dfrac{\mathrm{d}v_1(1)}{\mathrm{d}\xi}\\[2ex] \dfrac{\mathrm{d}v_2(-1)}{\mathrm{d}\xi}\end{pmatrix}. \tag{6.3}$$

Solutions of the equation $F(L_2,(v_1,v_2))=0$ correspond to the steady states of our model. Hence, we aim to find nontrivial solutions of (2.10) by studying bifurcations of (6.3) from the zero steady state solution at the bifurcation point $L_2=\bar L_2$, defined in (4.7).

The map F is continuous in v, twice Fréchet differentiable in v, and $F(L_2,(0,0))=0$ for all $L_2\geq 0$. We apply the local bifurcation theorem from [10].

Step 1: We determine the dimension of the null space of $\nabla_v F(\bar L_2,(0,0))$.

Standard calculations give us the Fréchet derivative of F at the bifurcation point $(L_2,(v_1,v_2)) = (\bar{L}_2,(0,0))$ as

$$\nabla_v F(\bar{L}_2,(0,0))[\phi] = \begin{pmatrix} D\frac{\mathrm{d}^2\phi_1}{\mathrm{d}\xi^2} + L_1^2\frac{\mathrm{d}H_1(0)}{\mathrm{d}v_1}\phi_1 \\ \frac{\mathrm{d}^2\phi_2}{\mathrm{d}\xi^2} + \bar{L}_2^2\frac{\mathrm{d}H_2(0)}{\mathrm{d}v_2}\phi_2 \\ \phi_1(0) - \phi_2(0) \\ \frac{\mathrm{d}\phi_2(0)}{\mathrm{d}\xi} - \frac{L_2}{L_1}\frac{\mathrm{d}\phi_1(0)}{\mathrm{d}\xi} \\ \frac{\mathrm{d}\phi_1(1)}{\mathrm{d}\xi} \\ \frac{\mathrm{d}\phi_2(-1)}{\mathrm{d}\xi} \end{pmatrix} = \begin{pmatrix} D\frac{\mathrm{d}^2\phi_1}{\mathrm{d}\xi^2} + RL_1^2\phi_1 \\ \frac{\mathrm{d}^2\phi_2}{\mathrm{d}\xi^2} - A\bar{L}_2^2\phi_2 \\ \phi_1(0) - \phi_2(0) \\ \frac{\mathrm{d}\phi_2(0)}{\mathrm{d}\xi} - \frac{\bar{L}_2}{L_1}\frac{\mathrm{d}\phi_1(0)}{\mathrm{d}\xi} \\ \frac{\mathrm{d}\phi_1(1)}{\mathrm{d}\xi} \\ \frac{\mathrm{d}\phi_2(-1)}{\mathrm{d}\xi} \end{pmatrix}, \tag{6.4}$$

where we have substituted the expressions for $H_i'(0)$ from our standard examples.

The null space, $N\left(\nabla_v F(\bar{L}_2,(0,0))\right)$, of $\nabla_v F(\bar{L}_2,(0,0))$ is therefore given by:

$$\left\{ \phi \in W : \begin{cases} D\frac{\mathrm{d}^2\phi_1}{\mathrm{d}\xi^2} + RL_1^2\phi_1 = 0; \\ \frac{\mathrm{d}^2\phi_2}{\mathrm{d}\xi^2} - A\bar{L}_2^2\phi_2 = 0; \\ \phi_1(0) = \phi_2(0),\ \frac{\mathrm{d}\phi_2(0)}{\mathrm{d}\xi} = \frac{\bar{L}_2}{L_1}\frac{\mathrm{d}\phi_1(0)}{\mathrm{d}\xi},\ \frac{\mathrm{d}\phi_2(-1)}{\mathrm{d}\xi} = 0,\ \frac{\mathrm{d}\phi_1(1)}{\mathrm{d}\xi} = 0. \end{cases} \right\}$$
$$= \mathrm{span}\{\psi\},$$

where ψ is the eigenfunction associated to the (simple) eigenvalue $\sigma_1(\bar{L}_2) = 0$ of (6.10). Since ψ is nonzero, $\dim(N(\nabla_v F(\bar{L}_2,(0,0)))) = 1$.

Step 2: We prove that the codimension of the range of $\nabla_v F(\bar{L}_2,(0,0))$ is 1.

For a bounded operator, the dimension of the null space of its adjoint operator is equal to the codimension of its range. We define the right-hand side of (6.4) as an operator $T : W \times \mathbb{R}^8 \to X \times \mathbb{R}^4$, show that it is bounded and determine its adjoint $T^\star$. We consider $\mathbb{R}^n$ with his standard inner product and define the inner product on X by

$$(\varphi,\phi)_X = \frac{\bar{L}_2}{DL_1}\int_0^1 \varphi_1\phi_1 \mathrm{d}\xi + \int_{-1}^0 \varphi_2\phi_2 \mathrm{d}\xi.$$

Let $\Phi \in W \times \mathbb{R}^8$ with

$$\Phi = \begin{pmatrix} \phi_1 & \phi_2 & \phi_1(0) & \phi_2(0) & \phi_1'(0) & \phi_2'(0) & \phi_1(1) & \phi_2(-1) & \phi_1'(1) & \phi_2'(1) \end{pmatrix}^\top$$

and $G = (g_1, g_2, a, b, c, d) \in X \times \mathbb{R}^4$. First, we show that T is a bounded operator. We have that:

$$\|T\Phi\|^2_{X\times\mathbb{R}^4} = \frac{\bar{L}_2}{DL_1}\int_0^1 \left|D\phi_1'' + RL_1^2\phi_1\right|^2 \mathrm{d}\xi + \int_{-1}^0 \left|\phi_2'' - A\bar{L}_2^2\phi_2\right|^2 \mathrm{d}\xi + (\phi_1(0) - \phi_2(0))^2 + \left(\phi_2'(0) - \frac{\bar{L}_2}{L_1}\phi_1'(0)\right)^2 + (\phi_1'(1))^2 + (\phi_2'(-1))^2 . \tag{6.5}$$

Next, we find a bound for each expression of (6.5). Using Cauchy's inequality, we have that:

$$\begin{aligned}\int_0^1 \left|D\phi_1'' + RL_1^2\phi_1\right|^2 \mathrm{d}\xi &\le D^2\|\phi_1''\|^2_{L^2} + R^2L_1^4\|\phi_1\|^2_{L^2} + 2DRL_1^2\|\phi_1\|_{L^2}\|\phi_1''\|_{L^2} \\ &\le D^2\|\phi_1''\|^2_{L^2} + R^2L_1^4\|\phi_1\|^2_{L^2} + DRL_1^2\left(\|\phi_1''\|^2_{L^2} + \|\phi_1\|^2_{L^2}\right).\end{aligned}$$

Therefore, we have the estimate

$$\int_0^1 \left|D\phi_1{}'' + RL_1^2\phi_1\right|^2 \mathrm{d}\xi \le \left(D^2 + R^2L_1^4 + 2DRL_1^2\right)\left(\|\phi_1\|^2_{L^2} + \|\phi_1{}''\|^2_{L^2}\right).$$

Similar steps give

$$\begin{aligned}\left(\phi_2'(0) - \frac{\bar{L}_2}{L_1}\phi_1'(0)\right)^2 &= (\phi_2'(0))^2 + \left(\frac{\bar{L}_2}{L_1}\phi_1'(0)\right)^2 - 2\frac{\bar{L}_2}{L_1}\phi_2'(0)\phi_1'(0) \\ &\le 2(\phi_2'(0))^2 + 2\left(\frac{\bar{L}_2}{L_1}\right)^2(\phi_1'(0))^2 \\ &\le \left(2 + 2\left(\frac{\bar{L}_2}{L_1}\right)^2\right)\left[(\phi_2'(0))^2 + (\phi_1'(0))^2\right].\end{aligned}$$

The other components can be estimated similarly. Therefore,

$$\begin{aligned}\|T\Phi\|^2_{X\times\mathbb{R}^4} &\le \left(D^2 + R^2L_1^4 + 2DRL_1^2\right)\frac{\bar{L}_2}{DL_1}\left(\|\phi_1\|^2_{L^2} + \|\phi_1''\|^2_{L^2}\right) \\ &\quad + \left(1 + 2A\bar{L}_2^2 + A^2\bar{L}_2^4\right)\left(\|\phi_2\|^2_{L^2} + \|\phi_2{}''\|^2_{L^2}\right) \\ &\quad + \left(6 + 2\left(\frac{\bar{L}_2}{L_1}\right)^2\right)\left[(\phi_1(0))^2 + (\phi_2(0))^2 + (\phi_2'(0))^2 + \left(\frac{\bar{L}_2}{L_1}\phi_1'(0)\right)^2\right. \\ &\quad \left. + (\phi_1'(1))^2 + (\phi_2'(-1))^2\right] \\ &\le C_1\|(\phi_1,\phi_2)\|^2_W + C_2\|\Phi\|^2 .\end{aligned}$$

Hence,

$$\|T\Phi\|^2_{X\times\mathbb{R}^4} \le C\|\Phi\|^2_{W\times\mathbb{R}^8},$$

where $C = C_1 + C_2$, with $C_1 = D^2 + R^2L_1^4 + 2DRL_1^2 + 1 + 2A\bar{L}_2^2 + A^2\bar{L}_2^4$ and $C_2 = 6 + 2(\bar{L}_2/L_1)^2$.

Next, we compute the adjoint operator of T in the standard way. We have that:

$$
\begin{aligned}
(T\Phi, G) &= \frac{\bar{L}_2}{DL_1}\int_0^1 \left[D\phi_1'' + RL_1^2\phi_1\right] g_1 \mathrm{d}\xi + \int_{-1}^0 \left[\phi_2'' - A\bar{L}_2^2\phi_2\right] g_2 \mathrm{d}\xi + a\left(\phi_1(0) - \phi_2(0)\right) \\
&\quad + b\left(\phi_2'(0) - \frac{\bar{L}_2}{L_1}\phi_1'(0)\right) + c\phi_1'(1) + d\phi_2'(-1) \\
&= \frac{\bar{L}_2}{DL_1}\int_0^1 \phi_1\left[Dg_1'' + RL_1^2 g_1\right] \mathrm{d}\xi + \int_{-1}^0 \phi_2\left[g_2'' - A\bar{L}_2^2 g_2\right] \mathrm{d}\xi \\
&\quad + \frac{\bar{L}_2}{L_1}\left([g_1\phi_1']_0^1 - [\phi_1 g_1']_0^1\right) + [g_2\phi_2']_{-1}^0 - [\phi_2 g_2']_{-1}^0 + a\left(\phi_1(0) - \phi_2(0)\right) \\
&\quad + b\left(\phi_2'(0) - \frac{\bar{L}_2}{L_1}\phi_1'(0)\right) + c\phi_1'(1) + d\phi_2'(-1) \\
&= \frac{\bar{L}_2}{DL_1}\int_0^1 \phi_1\left[Dg_1'' + RL_1^2 g_1\right] \mathrm{d}\xi + \int_{-1}^0 \phi_2\left[g_2'' - A\bar{L}_2^2 g_2\right] \mathrm{d}\xi + \frac{\bar{L}_2}{L_1} g_1(1)\phi_1'(1) \\
&\quad - \frac{\bar{L}_2}{L_1} g_1(0)\phi_1'(0) - \frac{\bar{L}_2}{L_1}\phi_1(1)g_1'(1) + \frac{\bar{L}_2}{L_1}\phi_1(0)g_1'(0) + g_2(0)\phi_2'(0) - g_2(-1)\phi_2'(-1) \\
&\quad - \phi_2(0)g_2'(0) + \phi_2(-1)g_2'(-1) + a\phi_1(0) - a\phi_2(0) + b\phi_2'(0) - b\frac{\bar{L}_2}{L_1}\phi_1'(0) + c\phi_1'(1) \\
&\quad + d\phi_2'(-1)
\end{aligned}
$$

$$
\begin{aligned}
&= \frac{\bar{L}_2}{DL_1}\int_0^1 \phi_1\left[Dg_1'' + RL_1^2 g_1\right] \mathrm{d}\xi + \int_{-1}^0 \phi_2\left[g_2'' - A\bar{L}_2^2 g_2\right] \mathrm{d}\xi + \left(a + \frac{\bar{L}_2}{L_1}g_1'(0)\right)\phi_1(0) \\
&\quad + \left(-a - g_2'(0)\right)\phi_2(0) + \left(-\frac{\bar{L}_2}{L_1}g_1(0) - b\frac{\bar{L}_2}{L_1}\right)\phi_1'(0) + \left(b + g_2(0)\right)\phi_2'(0) \\
&\quad - \frac{\bar{L}_2}{L_1}\phi_1(1)g_1'(1) + \phi_2(-1)g_2'(-1) + \left(c + \frac{\bar{L}_2}{L_1}g_1(1)\right)\phi_1'(1) + \left(d - g_2(-1)\right)\phi_2'(-1).
\end{aligned}
$$

Hence, we have $(T\Phi, G) = (\Phi, T^\star G)$, where

$$
T^\star G = \Bigg(\; Dg_1'' + RL_1^2 g_1 \quad g_2'' - A\bar{L}_2^2 g_2 \quad a + \frac{\bar{L}_2}{L_1}g_1'(0) \quad -a - g_2'(0) \quad -\frac{\bar{L}_2}{L_1}g_1(0) - b\frac{\bar{L}_2}{L_1}
$$

$$
b + g_2(0) \quad -\frac{\bar{L}_2}{L_1}g_1'(1) \quad g_2'(-1) \quad c + \frac{\bar{L}_2}{L_1}g_1(1) \quad d - g_2(-1) \; \Bigg)^\top.
$$

Next, we find the null space of $T^\star$. We have that: $T^\star G = 0 \Longleftrightarrow$

$$\begin{cases} Dg_1'' + RL_1^2 g_1 = 0 \\ g_2'' - A\bar{L}_2^2 g_2 = 0 \\ \begin{cases} a + g_1'(0) = 0 \\ -a - g_2'(0) = 0 \end{cases} \Longrightarrow \begin{cases} g_1'(0) = g_2'(0) \\ a = -g_2'(0) \end{cases} \\ \begin{cases} -\dfrac{\bar{L}_2}{L_1} g_1(0) - b\dfrac{\bar{L}_2}{L_1} = 0 \\ b + g_2(0) = 0 \end{cases} \Longrightarrow \begin{cases} g_1(0) = g_2(0) \\ b = -g_2(0) \end{cases} \\ -g_1'(1) = 0 \Longrightarrow g_1'(1) = 0 \\ g_2'(-1) = 0 \\ c + \dfrac{\bar{L}_2}{L_1} g_1(1) = 0 \Longrightarrow c = -\dfrac{\bar{L}_2}{L_1} g_1(1) \\ d - g_2(-1) = 0 \Longrightarrow d = g_2(-1) \end{cases} \Longrightarrow \begin{cases} Dg_1'' + RL_1^2 g_1 = 0 \\ g_2'' - A\bar{L}_2^2 g_2 = 0 \\ g_1(0) = g_2(0) \\ g_1'(0) = g_2'(0) \\ g_1'(1) = 0 \\ g_2'(-1) = 0 \\ a = -g_2'(0) \\ b = -g_2(0) \\ c = -\dfrac{\bar{L}_2}{L_1} g_1(1) \\ d = g_2(-1) \end{cases}$$

Therefore,

$$N(T^\star) = \operatorname{span}\left\{ \left(\psi_1, \psi_2, -\psi_2'(0), -\psi_2(0), -\frac{\bar{L}_2}{L_1}\psi_1(1), \psi_2(-1) \right) \right\}$$

and $\dim(N(T^\star)) = 1$. Since T is bounded, we obtain $\dim(N(T^\star)) = \operatorname{codim}(R(T)) = 1$, where R denotes the range of the operator.

Step 3: We show that

$$\frac{\mathrm{d}\nabla_v F}{\mathrm{d}L_2}(\bar{L}_2, (0,0))[\psi] \notin R(\nabla_v F(\bar{L}_2, (0,0))),$$

where $\psi \in N(\nabla_v F(\bar{L}_2, (0,0)))$.

We start by determining the expression of $R(\nabla_v F(\bar{L}_2, (0,0)))$. Since T is a bounded operator, the range of T is equal to the orthogonal space of the null space of its adjoint. Let $\Psi^\star \in N(T^\star)$, then

$$\begin{aligned} R(\nabla_v F(\bar{L}_2, (0,0))) &= \left\{ G = (g_1, g_2, a, b, c, d) \in X \times \mathbb{R}^4 \text{ such that } (\Psi^\star, G)_{X \times \mathbb{R}^4} = 0 \right\} \\ &= \left\{ G = (g_1, g_2, a, b, c, d) \in X \times \mathbb{R}^4 \text{ such that } l(g_1, g_2, a, b, c, d) = 0 \right\}, \end{aligned}$$

where l is defined by

$$l(g_1, g_2, a, b, c, d) = \frac{\bar{L}_2}{DL_1} \int_0^1 g_1\psi_1 + \int_{-1}^0 g_2\psi_2 - a\psi_2'(0) - b\psi_2(0) - c\frac{\bar{L}_2}{L_1}\psi_1(1) + d\psi_2(-1). \tag{6.6}$$

To show that $\frac{\mathrm{d}\nabla_v F}{\mathrm{d}L_2}(\bar{L}_2,(0,0))[\psi] \notin R(\nabla_v F(\bar{L}_2,(0,0)))$, we pick $\psi \in N(\nabla_v F(\bar{L}_2,(0,0)))$. We have that:

$$\begin{aligned}\frac{\mathrm{d}\nabla_v F}{\mathrm{d}L_2}(\bar{L}_2,(0,0))[\psi] &= \begin{pmatrix} 0 & 2\bar{L}_2\frac{\mathrm{d}H_2(0)}{\mathrm{d}v_2}\psi_2 & 0 & -\frac{1}{L_1}\psi_1'(0) & 0 & 0 \end{pmatrix}^\top \\ &= \begin{pmatrix} 0 & -2A\bar{L}_2\psi_2 & 0 & -\frac{1}{L_1}\psi_1'(0) & 0 & 0 \end{pmatrix}^\top,\end{aligned}$$

and

$$l\left(\frac{\mathrm{d}\nabla_v F}{\mathrm{d}L_2}(\bar{L}_2,(0,0))[\psi]\right) = -2A\bar{L}_2\int_{-1}^{0}\psi_2^2 + \psi_2(0)\frac{1}{L_1}\psi_1'(0).$$

We will later explicitly calculate the eigenfunction ψ and then evaluate this expression to find that it is indeed nonzero; see (6.9) and (6.14). We conclude that

$$\frac{\mathrm{d}\nabla_v F}{\mathrm{d}L_2}(\bar{L}_2,(0,0))[\psi] \notin R(\nabla_v F(\bar{L}_2,(0,0))).$$

Based on Steps 1–3, we apply Theorem 1.7 from [10] (see also Lemma 1.1 in [11]) and find: if Z is any complement of $N(\nabla_v F(\bar{L}_2,(0,0)))$ in W, the solutions of the equation $F(L_2,(v_1,v_2)) = 0$ near $\big(\bar{L}_2,(0,0)\big)$ consist precisely of the curves $(v_1,v_2) = (0,0)$ and $(L_2(s),(v_1(s),v_2(s))$, $s \in I = (-\delta,\delta)$. The functions $(L_2(s),(v_1(s),v_2(s))$ are $\mathcal{C}^1$ functions such that $L_2(0) = \bar{L}_2$, $(v_1(0),v_2(0)) = (0,0)$ and $(v_1'(0),v_2'(0)) = (\psi_1,\psi_2)$. Furthermore, $(v_1(s),v_2(s)) = (s\psi_1 + sz_1(s), s\psi_2 + sz_2(s))$, where (ψ_1,ψ_2) is the positive eigenfunction associated to $\sigma_1(\bar{L}_2)$, and $z(0) = z'(0) = 0$.

Step 4: We compute the formula for the direction of the bifurcation.

Shi provides this formula without details [29]. Here, we give the details. Following the original proof in [10], we define:

$$H(s,L_2(s),z(s)) = \begin{cases} s^{-1}F(L_2, s\psi + sz), & \text{if } s \neq 0, \\ \\ \nabla_v F(\bar{L}_2,(0,0))[\psi + z], & \text{if } s = 0. \end{cases}$$

By definition, $H(s,L_2(s),z(s)) = 0$. We differentiate this expression to find

$$H_s(s,L_2(s),z(s))\Big|_{s=0} + L_2'(s)H_{L_2}(s,L_2(s),z(s))\Big|_{s=0} + z'(s)H_z(s,L_2(s),z(s))\Big|_{s=0} = 0.$$

Since $z'(0) = 0$ (see above), the last of these three terms vanishes. For the second term, we calculate

$$\begin{aligned}&\lim_{h\to 0}\frac{H(0,L_2(0)+h,z(0)) - H(0,L_2(0),z(0))}{h} \\ =&\lim_{h\to 0}\frac{\nabla_v F(\bar{L}_2+h,(0,0))[\psi + z(0)] - \nabla_v F(\bar{L}_2,(0,0))[\psi + z(0)]}{h} \\ =&\frac{\mathrm{d}\nabla_v F}{\mathrm{d}L_2}(\bar{L}_2,(0,0)).\end{aligned}$$

The first term becomes

$$\begin{aligned}
&\lim_{h\to 0}\frac{H(h,L_2(0),z(0))-H(0,L_2(0),z(0))}{h}\\
=&\lim_{h\to 0}\frac{\frac{1}{h}F(\bar{L}_2,h(\psi+z(0)))-\nabla_v F(\bar{L}_2,(0,0))[\psi+z(0)]}{h}\\
=&\lim_{h\to 0}\frac{F(\bar{L}_2,h(\psi+z(0)))-h\nabla_v F(\bar{L}_2,(0,0))[\psi+z(0)]}{h^2}\\
=&\lim_{h\to 0}\frac{F(\bar{L}_2,(0,0)+h(\psi+z(0)))-F(\bar{L}_2,(0,0))-h\nabla_v F(\bar{L}_2,(0,0))[\psi+z(0)]}{h^2}\\
=&\lim_{h\to 0}\frac{\frac{1}{2}h^2\Delta_v F(\bar{L}_2,(0,0))[\psi+z(0)][\psi+z(0)]+\mathcal{O}(h^3)}{h^2}\\
=&\frac{1}{2}\Delta_v F(\bar{L}_2,(0,0))[\psi][\psi].
\end{aligned}$$

Hence, the above expression becomes

$$\frac{1}{2}\Delta_v F(\bar{L}_2,(0,0))[\psi][\psi]+L_2'(0)\frac{\mathrm{d}\nabla_v F}{\mathrm{d}L_2}(\bar{L}_2,(0,0))=0 \tag{6.7}$$

We want to solve this equation for $L_2'(0)$.

We begin with the second derivative of F. Since

$$\begin{aligned}
F_{1v}(v_1+\varphi_1)-F_{1v}(v_1)&=D\phi_1''+L_1^2\frac{\mathrm{d}H_1(v_1+\varphi_1)}{\mathrm{d}v}\phi_1-D\phi_1''+L_1^2\frac{\mathrm{d}H_1(v_1)}{\mathrm{d}v}\phi_1\\
&=L_1^2\phi_1\left(\frac{\mathrm{d}H_1(v_1+\varphi_1)}{\mathrm{d}v}-\frac{\mathrm{d}H_1(v_1)}{\mathrm{d}v}\right)=L_1^2\phi_1\varphi_1\frac{\mathrm{d}^2H_1(v_1)}{\mathrm{d}v^2},
\end{aligned}$$

we have

$$\Delta_v F(L_2,(v_1,v_2))[\phi][\varphi]=\begin{pmatrix} L_1^2\phi_1\varphi_1\dfrac{\mathrm{d}^2H_1(v_1)}{\mathrm{d}v^2} & L_2^2\phi_2\varphi_2\dfrac{\mathrm{d}^2H_2(v_2)}{\mathrm{d}v^2} & 0 & 0 & 0 & 0\end{pmatrix}^\top.$$

At the bifurcation point $(L_2,(v_1,v_2))=(\bar{L}_2,(0,0))$, we obtain

$$\Delta_v F(\bar{L}_2,(0,0))[\phi][\varphi]=\begin{pmatrix} -\dfrac{2R}{A}L_1^2\phi_1\varphi_1 & 2(1+A)L_2^2\phi_2\varphi_2 & 0 & 0 & 0 & 0\end{pmatrix}^\top$$

We also have that

$$\begin{aligned}
\frac{\mathrm{d}\nabla_v F}{\mathrm{d}L_2}(\bar{L}_2,(0,0))[\psi]&=\begin{pmatrix} 0 & 2\bar{L}_2\dfrac{\mathrm{d}H_2(v_2)}{\mathrm{d}v_2}\psi_2 & 0 & -\dfrac{1}{L_1}\psi_1'(0) & 0 & 0\end{pmatrix}^\top\\
&=\begin{pmatrix} 0 & -2A\bar{L}_2\psi_2 & 0 & -\dfrac{1}{L_1}\psi_1'(0) & 0 & 0\end{pmatrix}^\top.
\end{aligned}$$

With this, (6.7) now becomes

$$\begin{aligned}
&\begin{pmatrix} -\dfrac{R}{A}L_1^2\psi_1^2 & (1+A)L_2^2\psi_2^2 & 0 & 0 & 0 & 0\end{pmatrix}^\top\\
&+L_2'(0)\begin{pmatrix} 0 & -2A\bar{L}_2\psi_2 & 0 & -\dfrac{1}{L_1}\psi_1'(0) & 0 & 0\end{pmatrix}^\top=0.
\end{aligned} \tag{6.8}$$

Applying l from 6.6 to (6.8) gives

$$\left(-\frac{\bar{L}_2}{DL_1}\int_0^1\frac{R}{A}L_1^2\psi_1^3\mathrm{d}\xi+\int_{-1}^0(1+A)L_2^2\psi_2^3\mathrm{d}\xi\right)+L_2'(0)\left(\int_{-1}^0-2A\bar{L}_2\psi_2^2\mathrm{d}\xi+\frac{1}{L_1}\psi_1'(0)\psi_2(0)\right)=0.$$

Finally, we are ready to solve for $L_2'(0)$ and obtain (after simplifying)

$$L_2'(0) = L_1\bar{L}_2\left(\frac{\frac{R}{AD}L_1\int_0^1\psi_1^3\mathrm{d}\xi - (1+A)L_2\int_{-1}^0\psi_2^3\mathrm{d}\xi}{\psi_1'(0)\psi_2(0) - 2AL_1\bar{L}_2\int_{-1}^0\psi_2^2\mathrm{d}\xi}\right). \tag{6.9}$$

The sign of $L_2'(0)$ will give the direction of the bifurcation. As the last step, we now calculate this expression.

The principal eigenvalue $\sigma_1(L_2)$ and its associated eigenfunction $\psi = (\psi_1, \psi_2)$ of the eigenvalue problem

$$\begin{cases} D\phi_1'' + RL_1^2\phi_1 = \sigma\phi_1, & \tilde{\xi} \in [0,1]; \\ \phi_2'' - AL_2^2\phi_2 = \sigma\phi_2, & \tilde{\xi} \in [-1,0]; \\ \phi_1(0) = \phi_2(0),\ \phi_2'(0) = \dfrac{L_2}{L_1}\phi_1'(0),\ \phi_2'(-1) = 0,\ \phi_1'(1) = 0, \end{cases} \tag{6.10}$$

satisfy (using the same method as in [30, 25])

$$\begin{cases} \sigma_1(\bar{L}_2) = 0 \text{ where } \bar{L}_2 = \dfrac{1}{\sqrt{A}}\tanh^{-1}\left[\sqrt{\dfrac{R}{AD}}\tan\left(\sqrt{\dfrac{R}{D}}L_1\right)\right] \\ \psi_1(\xi) = F_2\dfrac{\cosh\left(\sqrt{A}\bar{L}_2\right)}{\cos\left(\sqrt{\dfrac{R}{D}}L_1\right)}\cos\left(\sqrt{\dfrac{R}{D}}L_1\left(\xi-1\right)\right), \\ \psi_2(\xi) = F_2\cosh\left(\sqrt{A}\bar{L}_2\left(\xi+1\right)\right) \end{cases} \tag{6.11}$$

for some nonzero number F_2, with $\psi_1'(0) = F_2\sqrt{R/D}\,L_1\cosh\left(\sqrt{A}\,\bar{L}_2\right)\tan\left(\sqrt{R/D}\,L_1\right)$ and $\psi_2(0) = F_2\cosh\left(\sqrt{A}\,\bar{L}_2\right)$.

We observe that $\bar{L}_2$ exists if and only if $0 \le \sqrt{R/AD}\tan\left(\sqrt{R/D}\,L_1\right) < 1$, which implies that $0 \le L_1 < \sqrt{D/R}\arctan\left(\sqrt{AD/R}\right)$.

Calculating the numerator and denominator of the expression in (6.9) is now possible, but tedious, using the formulas for powers of trigonometric functions. We only show one such calculation explicitly here, namely for the first integral in the numerator of (6.9).

With $a = \sqrt{R/D}\,L_1$, we have that

$$\int_0^1\cos^3(a(\xi-1))\mathrm{d}\xi = \left[\frac{\sin(3a(\xi-1)) + 9\sin(a(\xi-1))}{12a}\right]_0^1 = \frac{\sin(3a) + 9\sin(a)}{12a}.$$

Thus,

$$\begin{aligned}\frac{R}{AD}L_1\int_0^1\psi_1^3\mathrm{d}\xi &= F_2^3\frac{\cosh^3\left(\sqrt{A}\bar{L}_2\right)}{\cos^3\left(\sqrt{\frac{R}{D}}L_1\right)}\frac{R}{AD}L_1\left(\frac{\sin\left(3\sqrt{\frac{R}{D}}L_1\right)+9\sin\left(\sqrt{\frac{R}{D}}L_1\right)}{12\sqrt{\frac{R}{D}}L_1}\right)\\ &= F_2^3\frac{\cosh^3\left(\sqrt{A}\bar{L}_2\right)}{\cos^3\left(\sqrt{\frac{R}{D}}L_1\right)}\frac{\sqrt{R/D}}{12A}\left(\sin\left(3\sqrt{\frac{R}{D}}L_1\right)+9\sin\left(\sqrt{\frac{R}{D}}L_1\right)\right)\\ &= \frac{\sqrt{R/D}}{12A}F_2^3\cosh^3\left(\sqrt{A}\bar{L}_2\right)\left(\frac{\sin\left(3\sqrt{\frac{R}{D}}L_1\right)}{\cos^3\left(\sqrt{\frac{R}{D}}L_1\right)}+9\frac{\tan\left(\sqrt{\frac{R}{D}}L_1\right)}{\cos^2\left(\sqrt{\frac{R}{D}}L_1\right)}\right).\end{aligned}$$

Using several trigonometric identities, we finally arrive at

$$\frac{R}{AD}L_1\int_0^1\psi_1^3\mathrm{d}\xi = \frac{\sqrt{R/D}}{A}F_2^3\frac{\left[\tan\left(\sqrt{\frac{R}{D}}L_1\right)+\frac{2}{3}\tan^3\left(\sqrt{\frac{R}{D}}L_1\right)\right]}{\left[1-\frac{R}{AD}\tan^2\left(\sqrt{\frac{R}{D}}L_1\right)\right]^{3/2}}. \tag{6.12}$$

A similar calculation can be carried out for the second integral in the numerator of (6.9). Combining the two leads to the following expression of the numerator:

$$Num = \frac{\sqrt{R/D}}{A}F_2^3\tan\left(\sqrt{\frac{R}{D}}L_1\right)\left(\frac{-A+\frac{2}{3}\left(1+\frac{R}{AD}+\frac{R}{D}\right)\tan^2\left(\sqrt{\frac{R}{D}}L_1\right)}{\left[1-\frac{R}{AD}\tan^2\left(\sqrt{\frac{R}{D}}L_1\right)\right]^{3/2}}\right). \tag{6.13}$$

Equally tedious calculations involving trigonometric identities for the denominator give us

$$\begin{aligned}Deno &= \frac{F_2^2\sqrt{\frac{R}{D}}L_1\tan\left(\sqrt{\frac{R}{D}}L_1\right)}{1-\frac{R}{AD}\tan^2\left(\sqrt{\frac{R}{D}}L_1\right)}-L_1F_2^2\left(A\bar{L}_2+\frac{\sqrt{\frac{R}{D}}\tan\left(\sqrt{\frac{R}{D}}L_1\right)}{1-\frac{R}{AD}\tan^2\left(\sqrt{\frac{R}{D}}L_1\right)}\right)\\ &= -AL_1\bar{L}_2F_2^2.\end{aligned} \tag{6.14}$$

Now, using (6.13) and (6.14), we find that

$$L_2'(0) = \frac{\sqrt{R/D}}{A}F_2\tan\left(\sqrt{\frac{R}{D}}L_1\right)\left(\frac{-A+\frac{2}{3}\left(1+\frac{R}{AD}+\frac{R}{D}\right)\tan^2\left(\sqrt{\frac{R}{D}}L_1\right)}{-A\left[1-\frac{R}{AD}\tan^2\left(\sqrt{\frac{R}{D}}L_1\right)\right]^{3/2}}\right). \tag{6.15}$$

The denominator of $L_2'(0)$ is always negative, but the numerator can change sign. We calculate the sign change as a function of L_1, the length of patch 1.

$$\begin{aligned} L_2'(0) = 0 &\Longrightarrow -A + \frac{2}{3}\left(1 + \frac{R}{AD} + \frac{R}{D}\right)\tan^2\left(\sqrt{\frac{R}{D}}L_1\right) = 0 \\ &\Longrightarrow \tan^2\left(\sqrt{\frac{R}{D}}L_1\right) = \frac{3A}{2\left(1 + \frac{R}{AD} + \frac{R}{D}\right)} \\ &\Longrightarrow L_1^\star = \sqrt{\frac{D}{R}}\arctan\left(\sqrt{\frac{3A^2D}{2\left(AD + R + AR\right)}}\right). \end{aligned}$$

Therefore, for $L_1 < L_1^\star$, we have $L_2'(0) > 0$, thus the bifurcation is backward and for $L_1 > L_1^\star$, we have $L_2'(0) < 0$, thus the bifurcation is forward.

7. Discussion

We considered a fairly general model for population dynamics in a two-patch landscape. We allowed for qualitatively different growth functions on the two patches (monostable or bistable). We established the existence of steady states and some of their qualitative properties by analyzing the phase plane of the corresponding steady-state system. This method allowed us to generalize the existence result proved in [27] for logistic growth function to all monostable functions. In the case of mixed monostable/bistable dynamics, we classified all monotone steady states and proved that all steady states can be obtained from these by concatenation of periodic orbits in the phase plane.

Our results apply to more general landscapes, for example to a protected area (core) surrounded by a non-hostile but lower-quality area (buffer) as in [5] or to an infinite periodic landscape as in [25] and [17] as follows. In the first case, denote the interval $[-L_1, L_1]$ as the core and an interval of length L_2 on either side of this as the buffer, with our discontinuous interface conditions at $\pm L_1$. Then any solution on the two patch landscape $[0, L_1] \cup [L_1, L_1 + L_2]$ with no-flux condition at $x = 0$ as studied here, can then be extended to a (symmetric) solution on the core-buffer landscape. Similarly, every periodic two-patch landscape with patch sizes $2L_1$ and $2L_2$ can be concatenated from the two-patch landscape $[0, L_1] \cup [L_1, L_1 + L_2]$ by reflection and periodicity. Hence, every steady state on $[0, L_1] \cup [L_1, L_1 + L_2]$ with no-flux boundary extends to a steady state on a the periodic landscape.

To study the stability of steady states, we analyzed the corresponding eigenvalue problem. As a result, we generalized some of the classical Sturm–Liouville theory to our setting. It will be an interesting challenge to try and generalize other aspects, for example the result that zeros of eigenfunctions interlace. In general, explicit calculations of stability are rarely possible, but the case of spatially constant solutions (under some conditions on parameters) allows for such calculations and gives interesting insights. We proved the existence of multiple stable states and the existence of nonconstant steady states by a combination of linear analysis, sub- and supersolution methods and bifurcation results.

We did not consider the case where both growth functions are bistable, but we expect that the methods that we developed here carry over to that case. In fact, our argument that the classification of steady states reduces to the classification of monotone states carries over directly. The phase-plane analysis will consist of more cases, namely the combinations of the phase portraits in Figures 1(b), 1(c) and 1(d), but the arguments will be the same. The linear stability analysis at constant states will also carry over. One big difference will be that the zero state will always be stable, so that no solution will bifurcate from it.

The appearance of a fold bifurcation is not too surprising in our model. Such bifurcations are often associated with strong Allee effects. However, when considered on a single patch, one of the two locally stable states is the zero state [20]. In our case, we have a fold bifurcation where both stable states are nonzero; see Figure 7(c). This opens the door to hysteresis. For example, if the population initially is on the lower positive stable solution branch (say for $L_2 = 1.5$), then decreasing L_2 will lead to increasing population densities until L_2 crosses the bifurcation, upon which the population will jump to the higher positive solution branch. Upon increasing L_2 again, the population will stay at that level and not decline to the lower original level any more.

Even though Allee effects are common in nature, their treatment in mathematical models for population dynamics is quite rare. This is due, to a large extent, to the difficulty of analyzing such models rigorously. Similarly, spatially explicit and heterogeneous models are less frequently studied than either spatially implicit or spatially explicit but homogeneous models. For example, the classical spatially explicit Allee effect model consists of a single patch [20], whereas the landmark models for spatially heterogeneous population dynamics explicitly exclude an Allee effect [14, 22, 30]. A spatially explicit model with Allee effect in two different patch types was analyzed in [26], but only via homogenization and by numerical simulation. Our work and results provide a new approach and insights. For example, Allee effects are typically considered dangerous for population persistence so that one would like to limit them in an effort to protect species. Hence, increasing the size of an adjacent patch without Allee effect seems to be a useful measure. Looking at Figures 6(a), 6(b) and 6(e) shows that this is indeed helpful to populations at small densities: the zero state is stable when the Allee patch is large und unstable when the non-Allee patch is large. However, at the same time, the total population density at the positive steady state between K_1 and K_2 decreases, i.e., a larger population declines. Hence, well-meant management actions could have unintended negative consequences.

Acknowledgments. The authors would like to thank Prof Victor LeBlanc for discussions on the bifurcation result. FL is grateful for funding through the Discovery Grants program by the Natural Sciences and Engineering Research Council of Canada (RGPIN-2016-04795).

References

[1] M. A Al-Gwaiz, *Sturm-Liouville Theory And Its Applications*, Springer, New York, USA, 2008.
[2] Y. Alqawasmeh and F. Lutscher, *Movement behaviour of fish, harvesting-induced habitat degradation and the optimal size of marine reserves*, Theoretical Ecology **12** (2019), 453–466.
[3] ———, *Persistence and spread of stage-structured populations in heterogeneous landscapes*, Journal of Mathematical Biology **78** (2019), 1485–1527.
[4] K. J. Brown, C. Cosner, and J. Fleckinger, *Principal eigenvalues for problems with indefinite weight function on* $\mathbf{R}^n$, Proceedings of the American Mathematical Society **109** (1990), 147–155.
[5] R. S. Cantrell and C. Cosner, *Diffusion models for population dynamics incorporating individual behavior at boundaries: applications to refuge design*, Theoretical Population Biology **55** (1999), 189–207.
[6] ———, *Spatial Ecology Via Reaction-Diffusion Equations*, Wiley, Chichester, UK, 2003.
[7] C. A. Cobbold and F. Lutscher, *Mean occupancy time: linking mechanistic movement models, population dynamics and landscape ecology to population persistence*, Journal of Mathematical Biology **68** (2014), 549–579.
[8] C. Cosner, *Existence of global solutions to a model of a myelinated nerve axon*, SIAM Journal on Mathematical Analysis **18** (1987), 703–710.
[9] F. Courchamp, L. Berec, and J. Gascoigne, *Allee Effects In Ecology And Conservation*, Oxford University Press, Oxford, UK, 2008.
[10] M. G. Crandall and P. H. Rabinowitz, *Bifurcation from simple eigenvalues*, Journal of Functional Analysis **8** (1971), 321–340.
[11] ———, *Bifurcation, perturbation of simple eigenvalues and linearized stability*, Archive of Rational Mechanics and Analysis **52** (1973), 161–180.

[12] J. T. Cronin, J . oddard, and R. Shivaji, *Effects of patch–matrix composition and individual movement response on population persistence at the patch level*, Bulletin of Mathematical Biology **81** (2019), 3933–3975.
[13] L. C. Evans, *Partial Differential Equations*, American Mathematical Society, Rhode Island, USA, 1998.
[14] H. I. Freedman, J. B. Shukla, and Y. Takeuchi, *Population diffusion in a two-patch environment*, Mathematical biosciences **95** (1989), 111–123.
[15] D. Gilbarg and N. S. Trudinger, *Elliptic Partial Differential Equations of Second Order*, Springer, New York, USA, 1977.
[16] F. Hamel, F. Lutscher, and M. Zhang, *Propagation and blocking in a two-patch reaction-diffusion model*, Journal de Mathématiques Pures et Appliquées **168** (2022), 213–267.
[17] ———, *Propagation phenomena in periodic patchy landscapes with interface conditions*, Journal of Dynamics and Differential Equations (2022), doi.org/10.1007/s10884–022–10134–5.
[18] L. Ketchemen Tchouaga, *Population Dynamics In Patchy Landscapes Under Monostable And Bistable Dynamics*, Ph.D. thesis, University of Ottawa, 2023.
[19] H. Kierstead and L. B. Slobodkin, *The size of water masses containing plankton blooms*, Journal of Marine Research **12** (1953), 141–147.
[20] M. Kot, *Elements of Mathematical Ecology*, Cambridge University Press, Cambridge, UK, 2001.
[21] J. Langebrake, L. Riotte-Lambert, C. W. Osenberg, and P. De Leenheer, *Differential movement and movement bias models for marine protected areas*, Journal of Mathematical Biology **64** (2012), 667–696.
[22] D. Ludwig, D. G. Aronson, and H. F. Weinberger, *Spatial patterning of the spruce budworm*, Journal of Mathematical Biology **8** (1979), 217–258.
[23] ———, *Spatial pattern of the spruce budworm*, Journal of Mathematical Biology **8** (1979), 217–25.
[24] G. Maciel, C. Cosner, R. S. Cantrell, and F. Lutscher, *Evolutionary stable movement strategies in reaction-diffusion models with edge behavior*, Journal of Mathematical Biology **80** (2020), 61–92.
[25] G. Maciel and F. Lutscher, *How individual movement response to habitat edge effects population persistence and spatial spread*, The American Naturalist **182** (2013), 42–52.
[26] ———, *Allee effects and population spread in patchy landscapes*, Journal of Biological Dynamics **9** (2015), 109–123.
[27] N. Zaker, L. Ketchemen, and F. Lutscher, *The effect of movement behavior on population density in patchy landscapes*, Bulletin of Mathematical Biology **82** (2020), doi.org/10.1007/s11538–019–00680–3.
[28] O. Ovaskainen and O. Cornell, *Biased movement at a boundary and conditional occupancy times for diffusion processes*, Journal of Applied Probability **40** (2003), 557–580.
[29] J. Shi, *Persistence and bifurcation of degenerate solutions*, Journal of Functionnal Analysis **169** (1999), 494–531.
[30] N. Shigesada, K. Kawasaki, and E. Teramoto, *Traveling periodic waves in heterogeneous environments*, Theoretical Population Biology **30** (1986), 143–160.
[31] N. Shigesada, K. Kawasaki, and H. F. Weinberger, *Spreading speeds of invasive species in a periodic patchy environment: effects of dispersal based on local information and gradient-based taxis*, Japan Journal of Industrial and Applied Mathematics **32** (2015), 675–705.
[32] J. G. Skellam, *Random dispersal in theoretical populations*, Biometrika **38** (1951), 196–218.
[33] P. C. Tobin, S. L. Whitmire, D. M. Johnson, O. N. Bjørnstad, and A. M. Liebhold, *Invasion speed is affected by geographical variation in the strength of allee effects*, Ecology Letters **10** (2007), 36–43.
[34] O. Vasilyeva, *Population dynamics in rivers networks: analysis of steady states*, Journal of Mathematical Biology **79** (2019), 63–100.
[35] O. Vasilyeva and F. Lutscher, *Population dynamics in rivers: analysis of steady states*, Canadian Applied Mathematics Quarterly **18** (2010), 439–469.
[36] B. Yurk and C. Cobbold, *Homogenization techniques for population dynamics in strongly heterogeneous landscapes*, Journal of Biological Dynamics **12** (2018), 171–193.

L. Ketchemen Tchouaga, corresponding author, Department of Mathematics and Statistics, University of Ottawa, Ottawa, ON, Canada.

Current address: Department of Mathematics and Statistics, McGill University, Montreal, QC, Canada.

Email address: ketchemen_laurence@yahoo.fr

F. Lutscher, Department of Mathematics and Statistics, and Department of Biology, University of Ottawa, Ottawa, ON, Canada.

Email address: frithjof.lutscher@uottawa.ca